NANO REVIEW

# Magnetic Iron Oxide Nanoparticles: Synthesis and Surface Functionalization Strategies

**Wei Wu · Quanguo He · Changzhong Jiang**

**Abstract** Surface functionalized magnetic iron oxide nanoparticles (NPs) are a kind of novel functional materials, which have been widely used in the biotechnology and catalysis. This review focuses on the recent development and various strategies in preparation, structure, and magnetic properties of naked and surface functionalized iron oxide NPs and their corresponding application briefly. In order to implement the practical application, the particles must have combined properties of high magnetic saturation, stability, biocompatibility, and interactive functions at the surface. Moreover, the surface of iron oxide NPs could be modified by organic materials or inorganic materials, such as polymers, biomolecules, silica, metals, etc. The problems and major challenges, along with the directions for the synthesis and surface functionalization of iron oxide NPs, are considered. Finally, some future trends and prospective in these research areas are also discussed.

**Keywords** Magnetic iron oxide NPs ·
Surface functionalization · Preparation · Application

W. Wu · C. Jiang (✉)
Department of Physics, Wuhan University, Wuhan 430072,
People's Republic of China
e-mail: czjiang@whu.edu.cn

W. Wu
e-mail: w.wu@163.com

Q. He
Key Laboratory of Green Packaging and Bio-Nanotechnology
Applications (Hunan Province), Hunan University of
Technology, Zhuzhou 412008, People's Republic of China
e-mail: hequanguo@163.com

## Introduction

Nanoparticle are submicron moieties (diameters ranging from 1 to 100 nm according to the used term, although there are examples of NPs several hundreds of nanometers in size) made of inorganic or organic materials, which have many novel properties compared with the bulk materials [1]. On this basis, magnetic NPs have many unique magnetic properties such as superparamagnetic, high coercivity, low Curie temperature, high magnetic susceptibility, etc. Magnetic NPs are of great interest for researchers from a broad range of disciplines, including magnetic fluids, data storage, catalysis, and bioapplications [2–6]. Especially, magnetic ferrofluids and data storage are the applied researches that have led to the intergration of magnetic NPs in a myriad of commercial applications. Currently, magnetic NPs are also used in important bioapplications, including magnetic bioseparation and detection of biological entities (cell, protein, nucleic acids, enzyme, bacterials, virus, etc.), clinic diagnosis and therapy (such as MRI (magnetic resonance image) and MFH (magnetic fluid hyperthermia)), targeted drug delivery and biological labels. However, it is crucial to choose the materials for the construction of nano-structure materials and devises with adjustable physical and chemical properties. To this end, magnetic iron oxide NPs became the strong candidates, and the application of small iron oxide NPs in in vitro diagnostics has been practiced for nearly half a century [7]. In the last decade, increased investigations with several types of iron oxides have been carried out in the field of magnetic NPs (mostly includes the $Fe_3O_4$ magnetite, $Fe^{II}Fe^{III}_2O_4$, ferrimagnetic, superparamagnetic when the size is less than 15 nm), $\alpha$-$Fe_2O_3$ (hematite, weakly ferromagnetic or antiferromagnetic), $\gamma$-$Fe_2O_3$ (maghemite, ferrimagnetic), FeO

(wüstite, antiferromagnetic), $\varepsilon$-$Fe_2O_3$ and $\beta$-$Fe_2O_3$) [8], among which magnetite and maghemite is the very promising and popular candidates since its biocompatibility have already proven.

However, it is a technological challenge to control size, shape, stability, and dispersibility of NPs in desired solvents. Magnetic iron oxide NPs have a large surface-to-volume ratio and therefore possess high surface energies. Consequently, they tend to aggregate so as to minimize the surface energies. Moreover, the naked iron oxide NPs have high chemical activity, and are easily oxidized in air (especially magnetite), generally resulting in loss of magnetism and dispersibility. Therefore, providing proper surface coating and developing some effective protection strategies to keep the stability of magnetic iron oxide NPs is very important. These strategies comprise grafting of or coating with organic molecules, including small organic molecules or surfactants, polymers, and biomolecules, or coating with an inorganic layer, such as silica, metal or nonmetal elementary substance, metal oxide or metal sulfide. Practically, it is worthy that in many cases the protecting shells not only stabilize the magnetic iron oxide NPs, but can also be used for further functionalization.

In the following, we focus mainly on recent development and various strategies in the preparation, structure and magnetic properties of various surface functionalized strategies of magnetic iron oxide NPs and their corresponding applications, as well as the research advances on functionalizations of magnetic iron oxide NPs worldwide. Further the problems and major challenges still should be solved are pointed out, and the directions in these researches are also discussed.

## Synthesis of Iron Oxide NPs

In the last decades, much research has been developed to the synthesis of iron oxide NPs, and many reports have described efficient synthesis approaches to produce the shape-controlled, stable, biocompatible, and monodispersed iron oxide NPs. The most common methods including co-precipitation, thermal decomposition, hydrothermal synthesis, microemulsion, sonochemical synthesis, and sonochemical synthetic route can all be directed to the synthesis of high quality of iron oxide NPs. In addition, these NPs can also be prepared by the other methods such as electrochemical synthesis [9, 10], laser pyrolysis techniques [11], microorganism or bacterial synthesis (especially the Magnetotactic bacteria and iron reducing bacteria) [12, 13], etc. As follows, we try to present typical and recent examples for the discussions of each synthetic pathway and the corresponding formation mechanism.

### Co-Precipitation

The most conventional method for obtaining $Fe_3O_4$ or $\gamma$-$Fe_2O_3$ is by co-precipitation. This method consists of mixing ferric and ferrous ions in a 1:2 molar ratio in highly basic solutions at room temperature or at elevated temperature. The size and shape of the iron oxide NPs depends on the type of salt used (such as chlorides, sulfates, nitrates, perchlorates, etc.), the ferric and ferrous ions ratio, the reaction temperature, the PH value, ionic strength of the media, and the other reaction parameters (e.g. stirring rate, dropping speed of basic solution). Recently we have reported the co-precipitation synthesis of $Fe_3O_4$ NPs and their corresponding morphology, structure, and magnetic properties at different reaction temperature was investigated [14].

This method would critically affect the physical and chemical properties of the nanosized iron oxide particles. Generally, the saturation magnetization ($M_S$) values found in nanostructured materials are usually smaller than the corresponding bulk phase, provided that no change in ionic configurations occurs [15]. Accordingly, experimental value for $M_S$ in magnetic iron oxide NPs have been reported to span the 30–80 emu $g^{-1}$ range, lower than the bulk magnetic value 100 emu $g^{-1}$. In addition, $Fe_3O_4$ NPs are not very stable under ambient conditions and are easily oxidised to $Fe_2O_3$ or dissolved in an acidic medium. In order to avoid the possible oxidation in the air, the synthesis of $Fe_3O_4$ NPs must be done in an anaerobic conditions. Based on this point, $Fe_3O_4$ NPs can also be utilized to prepare the $Fe_2O_3$ NPs by oxidation or anneal treatment under oxygen atmosphere. And oxidation is not the important influence factor for $Fe_2O_3$ NPs due to its own chemical stability in alkaline or acidic environment.

However, this method generates particles with a wide particle size distribution, which requires secondary size selection sometimes. A wide particle size distribution will result in a wide range of blocking temperatures ($T_B$) due to $T_B$ depends on particle size and, therefore non-ideal magnetic behavior for many applications. Kang et al. [16] reported a synthesis of monodispersed, uniform, and narrow size distributional $Fe_3O_4$ NPs (the diameter of NPs was $8.5 \pm 1.3$ nm) by co-precipitation without surfactants, the reaction in an aqueous solution with a molar ratio of $Fe^{II}/Fe^{III} = 0.5$ and a pH $= 11$–$12$, and the colloidal suspensions of the magnetite can be then directly oxidized by aeration to form colloidal suspensions of $\gamma$-$Fe_2O_3$. In contrast, many recent publications have described efficient routes to obtain the monodispersed NPs, surfactants such as dextran or polyvinyl alcohol (PVA) can be added in the reaction media, or the particles can be coated in a subsequent step [17, 18]. Surfactants act as protecting agent for controlling particle size and stabilizing the colloidal dispersions.

Additionally, the disadvantage of these aqueous solution syntheses is that the high pH value of the reaction mixture

has to be adjusted in both the synthesis and purification steps, and the process toward uniformed and monodispersed NPs has only very limited success. On the other hand, wastewaters with very basic pH values are also generated in the experiment, which require subsequent treatments for protecting the environment.

## Thermal Decomposition

An organic solution phase decomposition route has been widely used in iron oxide NPs synthesis, and decomposition of Fe(cup)$_3$ (cup = N-nitrosophenylhydroxylamine), Fe(acac)$_3$ (acac = acetylacetonate), or Fe(CO)$_5$ followed by oxidation can lead to high-quality monodispersed iron oxide NPs, which usually requires relatively higher temperatures and a complicated operation.

Sun and Zeng [19] have reported a general decomposition approach for the synthesis of size-controlled monodispersed magnetite NPs based on high temperature (265 °C) reaction of Fe(acac)$_3$ in phenyl ether in the presence of alcohol, oleic acid, and oleylamine. With the smaller magnetite NPs as seeds, larger monodispersed magnetite NPs of up to 20 nm in diameter can be synthesized and dispersed into nonpolar solvent by seed-mediated growth method. The process does not require a size-selection procedure and is readily scaled up for mass production. The as-synthesized Fe$_3$O$_4$ nanoparticle assemblies can be transformed easily into γ-Fe$_2$O$_3$ NPs by annealing at high temperature (250 °C) and oxygen for 2 h.

Generally, direct decomposition of Fe(Cup)$_3$ single precursor can lead to monodispersed γ-Fe$_2$O$_3$ NPs [20]. The thermal decomposition of Fe(CO)$_5$ produces iron NPs and the following oxidation by a chemical reagent can also lead to monodispersed γ-Fe$_2$O$_3$ NPs [21]. For instance, Hyeon et al. [22] reported a synthesis of highly crystalline and monodispersed iron NPs without size-selection process by the thermal decomposition of iron pentacarbonyl in the presence of oleic acid at 100 °C. The resulting iron NPs were transformed to monodispersed γ-Fe$_2$O$_3$ nanocrystallites by controlled oxidation using trimethylamine oxide as a mild oxidant. Particle size can be varied from 4 to 16 nm by controlling the experimental parameters.

Although the thermal decomposition method has many advantages for producing highly monodispersed particles with a narrow size distribution, it has the big disadvantage that the resulting NPs are generally only dissolved in nonpolar solvents.

## Microemulsion

Microemulsion is a thermodynamically stable isotropic dispersion of two immiscible phases (water and oil) under the surfactant present, the surfactant molecules may form a monolayer at the interface between the oil and water, with the hydrophobic tails of the surfactant molecules dissolved in the oil phase and the hydrophilic head groups in the aqueous phase. As in the binary systems (water/surfactant or oil/surfactant), self-assembled structures of different types can be formed, ranging, for example, from (inverted) spherical and cylindrical micelles to lamellar phases and bicontinuous microemulsions, which may coexist with predominantly oil or aqueous phases [23]. In this sense, microemulsion and inverse micelles route can be employed for obtaining the shape- and size-controlled iron oxide NPs.

Particularly, water-in-oil (w/o) microemulsions are formed by well-defined nanodroplets of the aqueous phase, dispersed by the assembly of surfactant molecules in a continuous oil phase. Vidal-Vidal et al. [24] have reported the synthesis of monodisperse maghemite NPs by the one-pot microemulsion method. The spherical shaped particles, capped with a monolayer coating of oleylamine (or oleic acid), show a narrow size distribution of 3.5 ± 0.6 nm, are well crystallized and have high saturation magnetization values (76.3 Am$^2$/kg for uncoated NPs, 35.2 Am$^2$/kg for oleic acid coated NPs, and 33.2 Am$^2$/kg for oleylamine coated NPs). Moreover, the results show that oleylamine act as precipitating and capping agent. However, cyclohexylamine acts only as precipitating agent and does not avoid particle aggregation. Chin and Yaacob reported the synthesis of magnetic iron oxide NPs (less than 10 nm) via w/o microemulsion, furthermore, in comparison to the particles produced by Massart's procedure [25], particles produced by microemulsion technique were smaller in size and were higher in saturation magnetization [26].

However, despite the presence of surfactants, the aggregation of the produced NPs usually needs several washing processes and further stabilization treatments.

## Hydrothermal Synthesis

Iron oxide NPs with controlled size and shape are technologically important due to strong correlation between these parameters and magnetic properties. The microemulsion and thermal decomposition methods usually lead to complicated process or require relatively high temperatures. As an alternative, hydrothermal synthesis includes various wet-chemical technologies of crystallizing substance in a sealed container from the high temperature aqueous solution (generally in the range from 130 to 250 °C) at high vapor pressure (generally in the range from 0.3 to 4 MPa). This technique has also been used to grow dislocation-free single crystal particles, and grains formed in this process could have a better crystallinity than those from other processes, so hydrothermal synthesis is prone to obtain the highly crystalline iron oxide NPs.

Several authors have reported the synthesis of iron oxide NPs by hydrothermal method [27–30]. There are two major

methods according to whether or not use the specific surfactants. For example, Wang et al. [31] have reported a one-step hydrothermal process to prepare highly crystalline $Fe_3O_4$ nanopowders without using the surfactants. The nanoscale $Fe_3O_4$ powder (40 nm) obtained at 140 °C for 6 h possessed a saturation magnetization of 85.8 emu·g$^{-1}$, a little lower than that of the correspondent bulk $Fe_3O_4$ (92 emu·g$^{-1}$). It is suggested that the well-crystallized $Fe_3O_4$ grains formed under appropriate hydrothermal conditions should be responsible for the increased saturation magnetization in nanosized $Fe_3O_4$. On the contrary, Zheng et al. [32] reported a hydrothermal route for preparing $Fe_3O_4$ NPs with diameter of ca. 27 nm in the presence of a surfactant, sodium bis(2-ethylhexyl)sulfosuccinate (AOT). The magnetic properties of the NPs exhibited a superparamagnetic behavior at room temperature.

Moreover, hydrothermal treatment is one of the successful ways of growing crystals for iron oxide NPs. Recently Daou et al. [33] have reported that the magnetite particles with an average size of 39 nm and good monodispersity have been synthesized by co-precipitation at 70 °C from ferrous $Fe^{2+}$ and ferric $Fe^{3+}$ ions by a $N(CH_3)_4OH$ solution, followed by hydrothermal treatment at 250 °C. The magnetite NPs before the hydrothermal step display an average size of 12 nm and are highly oxidized when they are in contact with air. Additionally, hydrothermal synthesis is conductive to prepare the unusual iron oxide nanostructures such as iron oxide nanocubes [34], iron oxide hollow spheres [35], etc.

Sonochemical Synthesis

As a competitive alternative, the sonochemical method has been extensively used to generate novel materials with unusual properties. The chemical effects of ultrasound arise from acoustic cavitation, that is, the formation, growth, and implosive collapse of bubbles in liquid. The implosive collapse of the bubble generates a localized hotspot through adiabatic compression or shock wave formation within the gas phase of the collapsing bubble. The conditions formed in these hotspots have been experimentally determined, with transient temperatures of 5000 K, pressures of 1800 atm, and cooling rates in excess of $10^{10}$ K/s [36]. These extreme conditions were beneficial to form the new phase, and have a shear effect for agglomeration, which is prone to prepare the highly monodispersive NPs.

This method has been applied for the synthesis of various nanocomposites, and its versatility has been successfully demonstrated in iron oxide NPs preparation [37]. For instance, magnetite NPs can be simply synthesized by sonication of iron(II)acetate in water under an argon atmosphere. Vijayakumar et al. [38] reported a sonochemical synthetic route for preparing the pure nanometer-size $Fe_3O_4$ powder with particle size of ca. 10 nm. The prepared $Fe_3O_4$ NPs are superparamagnetic and its magnetization at room temperature is very low (<1.25 emu g$^{-1}$). Recently Pinkas et al. [39] developed a sonochemical synthetic method for preparing the amorphous nanoscopic iron oxide by sonolysis of $Fe(acac)_3$ under Ar with a small amount of added water. The organic content and the surface area of the $Fe_2O_3$ NPs can be controlled with an amount of water in the reaction mixture, and it increases from 48 m$^2$ g$^{-1}$ for dry solvent up to 260 m$^2$ g$^{-1}$ when wet Ar is employed. Such surface modified ultrasmall (1–2 nm) NPs exhibit an unrecorded low magnetic transition temperature of about 25 K, below this temperature they behave as speromagnetic, highly magnetically disordered systems with a high contribution of the surface anisotropy, and this speromagnetic behavior can be observed by Mössbauer spectra.

The five above mentioned synthetic methods have several advantages and disadvantages for preparing iron oxide NPs, respectively. In terms of size and morphology control of the iron oxide NPs, thermal decomposition and hydrothermal synthetic route seems the optimal method. For obtaining the water-soluble and biocompatible iron oxide NPs, co-precipitation often was employed, but this method presents low control of the particle shape, broad distributions of sizes and aggregation of particles. As a time-competitive alternative, sonochemical route can also be used to synthesis iron oxide NPs with unusually magnetic properties. In addition, it is noteworthy that some green chemical synthesis routes and biological synthesis routes have been reported for environment protection purposes. For example, recently Bharde et al. [12] reported the bacterium *Actinobacter* sp. is capable of synthesizing maghemite under aerobic conditions when reacted with the ferric chloride precursors. Moreover, maghemite NPs show superparamagnetic characteristics as expected. Therefore, as the enviromental protection and eco friendliness-competitive alternative, green chemistry and biological methods such as bacterially induced synthesis based synthesis of iron oxide NPs are important advances.

In the following sections, the recent development and various strategies for obtaining surface functionalized iron oxide NPs by organic and inorganic materials will be discussed.

**Surface Functionalization by Organic Materials**

In the preparation and storage of ferrofluids, the stability is of utmost importance. Organic compounds are often employed to passivate the surface of the iron oxide NPs during or after the preparing procedure to avoid agglomeration. The main reasons for magnetic iron oxide NPs

have hydrophobic surfaces with a large surface area-to-volume ratio if in the absence of any proper surface coating, and the hydrophobic interactions between the NPs will cause them to aggregate and form large clusters, resulting in increased particle size. Additionally, in order to expand the biological application scope of the iron oxide NPs, some biomolecules are also employed to enhance its biocompatibility.

In recent years, considerable efforts have been devoted to the design and controlled fabrication of nanostructured materials displaying specific functional properties. Organic compounds coated on iron oxide NPs offer a high potential application in several areas. The structure of organic compounds functionalized magnetic iron oxide NPs consists of two major parts: preserved the magnetic property of magnetic iron oxides and preserved the other properties of organic molecules. Generally, if iron oxides were always assumed as the core, its structure can roughly be divided into three types: core-shell, matrix, and shell$_a$-core-shell$_b$. As plotted in Fig. 1, coating an ensemble of iron oxide NPs by organic material yields core-shell nanostructure. In these structures, the cores may be any kind of iron oxide particles, such as magnetite or maghemite. Likewise, the shells may consist of any sort of materials including organic ones. Matrix structure includes two typical structures: mosaic and shell-core. Comparatively speaking, the shell-core structure consists of an organic compound NPs core and iron oxide particle shells. Iron oxide NPs may connect with the organic core by the interaction of chemical bonds. The mosaic structure comprising the shell layer was made of organic molecules coated to a lot of uniformly iron oxide magnetic NPs. Among the different matrixes that can be used to embed the NPs, polymers are of particular interest because of their wide range of properties. Furthermore, a shell layer made of organic molecules coated to a shell-core structurally functionalized iron oxide NPs that will form the shell$_a$-core-shell$_b$ structure, which occurs in many current reports and generally obtained by *layer-by-layer* technology. The shell$_a$ may be the polymer or biomolecules, likewise, the shell$_b$ can be the same or different functional materials. Moreover, multi-component conducting organic material systems with iron oxide NPs can be tailored to obtain desired mechanical properties besides novel electrical, magnetic, and optical properties.
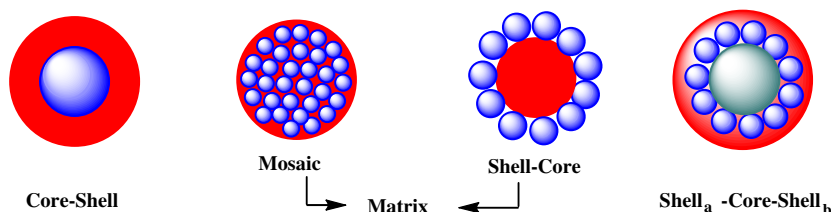
Organic compounds functionalized iron oxide NPs provide not only the basic magnetism characteristics of magnetic NPs, but also possess good biocompatibility and biodegradability of the functional organic materials. Moreover, organic moleculars can provide the ensemble functional reactive group, e.g. aldehyde groups, hydroxyl groups, carboxyl groups, amino groups, etc. It is crucial that their groups can link to the active biosubstance such as antibody, protein, DNA, enzyme, etc., for the further application. In the following section, the organic small molecules, macromolecules or polymer and biological molecules functionalized iron oxide NPs and the corresponding properties will be discussed.

Small Molecules and Surfactants

A suitable surface functionalization and choice of solvent are crucial to achieving sufficient repulsive interactions to prevent agglomeration so as to obtain a stable colloidal solution and further expand the scope of application. According to the surface characteristics of the functionalized NPs, small molecules or surfactants functionalized iron oxide NPs can be simply divided into three types: oil-soluble, water-soluble, and amphiphilic. Oil-soluble type refers to the surface of functionalized iron oxide NPs containing the molecular which have a weak attraction for the solvent environment, it is generally hydrophobic group, such as the fatty acid, alkyl phenol ($n = 6–10$, linear or branched). Conversely, water-soluble type refers to the surface of functionalized iron oxide NPs containing the chemical groups which have a strong attraction for the solvent environment, it is generally hydrophilic groups, such as the ammonium salt, polyol, lycine. Amphiphilic type refers to the surface of functionalized iron oxide NPs containing both hydrophilic and hydrophobic chemical groups, the main chain of these functionalized small molecules or surfactants showed concurrence of hydrophobic and hydrophilic structural regions, which also will make the functionalized NPs possess both oil-solubility and water-solubility, such as sulfuric lycine.

Oil-soluble type functionalization employed in order to prevent or decrease the agglomeration of iron oxide NPs and increase the stability give rise to the monodispersity, for instance, iron oxide NPs frequently dispersed in long-chain substance of hexadecane, the classic example being

Fig. 1 The representative structure of organic materials functionalized magnetic iron oxide NPs (if iron oxide NPs were always assumed as the core)



**Core-Shell**

**Mosaic**

**Shell-Core**

**Matrix**

**Shell$_a$ -Core-Shell$_b$**

oleic acid $(CH_3(CH_2)_7CH=CH(CH_2)_7CO_2H)$, which has a C18 tail with a cis-double-bond in the middle, forming a kink. Such kinks have been postulated as necessary for effective stabilization, and indeed stearic acid $(CH_3(CH_2)_{16}CO_2H)$ with no double-bond in its C18 tail, cannot stabilize the iron oxide NPs [7, 40–42]. Additionally, Oleic acid is widely used in ferrite nanoparticle synthesis because it can form a dense protective monolayer, thereby producing highly uniform and monodisperse particles. However, relative to the naked iron oxide NPs, the average diameter of functionalized NPs will increase in the range of 0–5 nm, and its saturation magnetization ($M_S$) almost unchanged.

Several authors have reported the magnetic iron oxide NPs coated or dispersed in the oil-soluble organic molecules. Shaoo et al. [43] have reported the surface-coated magnetite NPs with a 6–8 nm average diameter by oleic acid, lauric acid, dodecyl phosphonate, hexadecyl phosphonate, and dihexadecyl phosphate etc., they found that alkyl phosphonates and phosphates could be used for obtaining thermodynamically stable dispersions of magnetite NPs. The organic molecules' ligands seem to form a quasi-bilayer structure with the primary layer strongly bonded to the surface of the NPs. This study demonstrates that alkyl phosphonates and phosphates bind efficiently to iron oxide particle surfaces, the good biocompatibility of phosphonate and phosphate ligands may advance the utilization of encapsulated magnetic NPs in medical applications, such as MRI and other biophysical purposes. Bourlions et al. [44] have reported the synthesis of capped ultrafine $\gamma$-Fe$_2$O$_3$ NPs under anaerobic conditions by the thermal treatment of a hydrated iron(III) hydroxide caprylate gel in boiling tetraline and by retention of the organophilic mantle around the parent particle throughout the final solid. The capped particles, which possessed a spherical morphology and an average size of 4 nm, were easily solvated in organic solvents to provide stable and homogeneous magnetic organosols.

However, the oil-soluble type functionalized iron oxide NPs are relatively easy to prepare and control. Currently the mainly research focus are the synthesis of water-soluble type functionalized iron oxide NPs with water solubility (good disperse in aqueous environment, can not produce agglomeration), biological compatibility (good for protein, antibody, biotin, DNA etc., low cytotoxicity, low effect their activity), and biodegradability. Water-soluble functionalized iron oxide NPs can be widely utilized in bioseparation and biodetection.

Several routes were employed for obtaining the water-soluble functionalized iron oxide NPs. One method is to directly add the biocompatible small organic molecules such as amino acid [45], citric acid [43, 46], vitamin [47, 48], cyclodextrin [49–51], etc. during the synthesis

procedure. Recently Xia et al. [52] reported a facile synthetic approach for preparing water-soluble Fe$_3$O$_4$ NPs with a surrounded layer by use of polyethylene glycol nonylphenyl ether (NP5) and cyclodextrin (CD) in aqueous medium. Moreover, the author had also built nanostructured spherical aggregates (mosaic type structure) from individual functionalized NPs (core-shell type structure) and which can be tailored by the concentration of NP5 and CD. These mesoporous aggregates of magnetite NPs can be used in magnetic carrier technology. Though this direct method has many advantages, owing to small organic molecules do not have good stability especially in an alkaline or acidic environment, it often decomposes and results in the functionalized iron oxide NPs agglomeration. Furthermore, the morphology of functionalized iron oxide NPs often presents as an aggregate clusters.

Another method is to transform the oil-soluble type into water-soluble type functionalized iron oxide NPs, and the ligand-exchange reaction is the major approach to realize this aim [53]. Ligand exchange is a well-known method for tuning the surface properties of NPs. It involves adding an excess of ligand to the nanoparticle solution, which results in the displacement of the original ligand on the NPs' surface. Especially, ligand-exchange reactions on noble metal NPs, via the self-assembly of thiols, have been used for many years already [54, 55]. However, more recently, several groups have reported the use of ligand exchange to alter the surface properties of iron oxide NPs. Sun et al. [56] have prepared a monodispersed magnetite NPs with a tunable diameter range from 3 to 20 nm by the high temperature solution phase reaction of iron(III) acetylacetonate, Fe(acac)$_3$, with 1,2-hexadecanediol in the presence of oleic acid and oleylamine. And the hydrophobic NPs can be transformed into hydrophilic ones by mixing with bipolar surfactants such as tetramethylammonium 11-aminoundecanoate, allowing preparation of aqueous nanoparticle dispersions. Subsequently, as illustrated in Fig. 2, Lattuada and Hatton [57] reported that the oleic groups initially present on the above nanoparticle surfaces were replaced via ligand-exchange reaction with various capping agents bearing reactive hydroxyl moieties. They also found that particle sizes in the range of 6 to 11 nm can be tuned without using the seeded-growth process by simply varying the heating rate of the solution containing the nucleating particles. This route was proposed a flexible methodology for the preparation of various types of monodisperse, water-soluble magnetic NPs coated by different polymer brushes. A similar approach was used by Fan et al. [58] to prepare a water-dispersible $\gamma$-Fe$_2$O$_3$ NPs with narrow size distributions (13 ± 2 nm) via site-exchange reaction, and these NPs were superparamagnetic and stable without aggregation in a wide range of pH 3–9. Additionally, attachment of the biotin functionality onto

**Fig. 2** Scheme for the magnetic NPs functionalization procedure described in this work. Steps 1A and 1B: ligand-exchange reactions. Step 2: acylation of hydroxyl groups to prepare ATRP surface initiators. Step 3A: surface-initiated ring opening polymerization of L-lactide. Steps 3B: surface-initiated ATRP. Step 4: deprotection or additional reaction after polymerization. Step 5: graftiong of endfunctionalized PEG chains onto the nanoparticle surface using amidation chemistry. From [57]
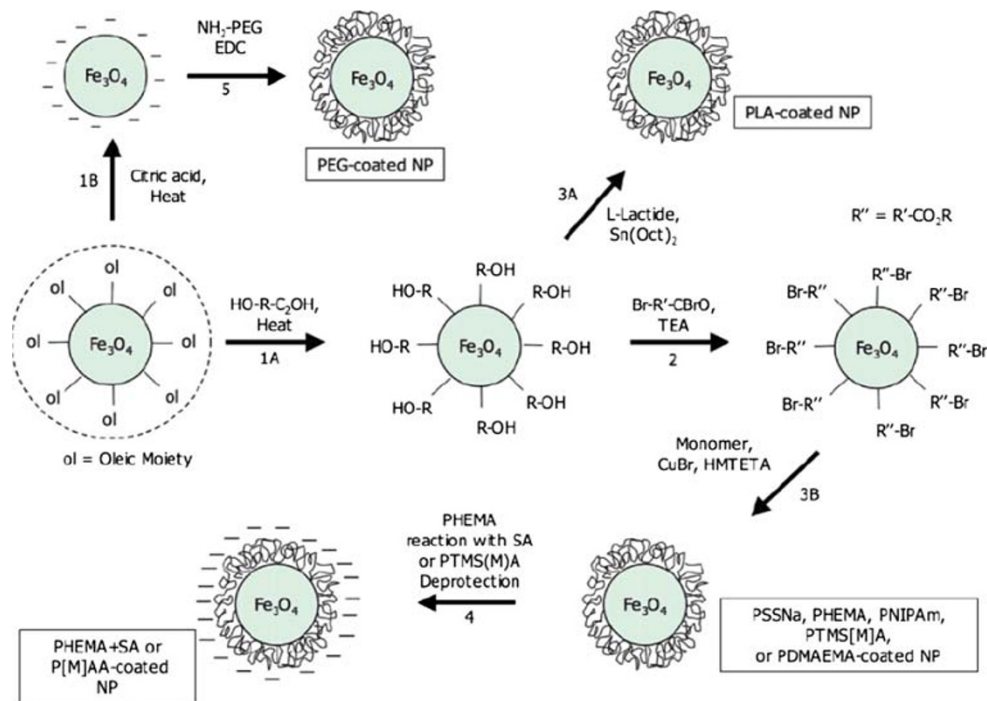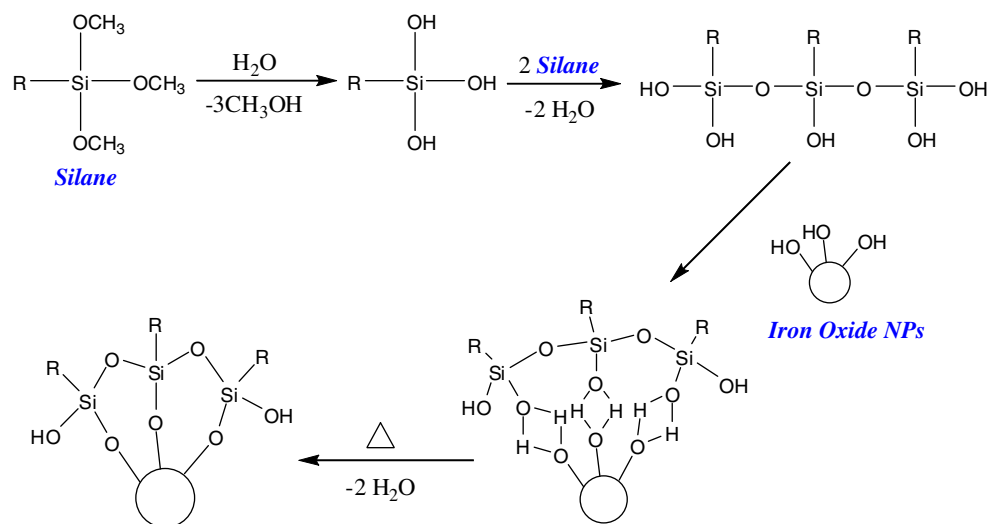


**Fig. 3** Physicochemical mechanism for modifying the silane agents on the surface of iron oxide NPs



the surfaces of our NPs enabled the magnetic affinity isolation of avidin–FITC from its incubation buffer with 96% efficiency. However, ligand-exchange reaction often contributes to the complicated operation and the difficulty of control exchange rate, these problems are urgent to be solved.

Moreover, the silane agent is often considered as a candidate for modifying on the surface of iron oxide NPs directly, for the advantages of the biocompatibility as well as high density of surface functional endgroups, and allowing for connecting to other metal, polymer or biomolecules [59, 60]. In general, silane-coated iron oxide NPs still maintains the physical characteristics of naked NPs with high saturation magnetization, the decrease value of

saturation magnetization often less than 10 emu g$^{-1}$. The 3-aminopropyltriethyloxysilane (APTES), p-aminophenyl trimethoxysilane (APTS), and mercaptopropyltriethoxysilane (MPTES) agents were mostly employed for providing the amino and sulfhydryl group, respectively. The physicochemical mechanism of the silane agent modifying on the surface of iron oxide NPs according to Arkles is depicted in Fig. 3 [61]. The hydroxyl groups on the iron oxide NPs surface reacted with the methoxy groups of the silane molecules leading to the formation of Si–O bonds and leaving the terminal functional groups available for immobilization the other substance.

We have prepared magnetite NPs with average diameter $25 \pm 5$ nm by modified chemical co-precipitation, and

silane bridged surface tailoring are exploited to obtain amino-coated and thiolated magnetite NPs via corresponding APTES and MPTES modification, respectively. The result reveals that the surface functionalized magnetic particles have a slight dimensional increase in average diameter while retain almost original saturation magnetization; APTES is prone to maintain the morphology of the magnetite NPs, but MPTES has an outstanding hypochromic effect though it caused a slight decrease in the saturation magnetization. The finding is of practical significance for magnetic NPs applications associated with bioconjugation, target carriers, and biosensing [62]. In addition, silanes were found to render the iron oxide NPs highly stable and water-dispersible, and it was also found to form a protective layer against mild acid and alkaline environments. Moreover, silane ligand-exchange reaction can make the hydrophobic iron oxide NPs into water-dispersible [63].

Polymers

Although most studies have focused on the development of small organic molecules and surfactants coating up to now, recently polymers functionalized iron oxide NPs are receiving more and more attention, owing to the advantages of polymers coating will increase repulsive forces to balance the magnetic and the *van der Waals* attractive forces acting on the NPs. In addition, polymers coating on the surface of iron oxide NPs offer a high potential in the application of several fields. Moreover, polymer functionalized iron oxide NPs have been extensively investigated due to interest in their unique physical or chemical properties. To make use of these materials for fundamental or applied research, access to well-defined NPs samples whose properties can be "tuned" through chemical

modification is necessary. In a number of cases it has now been shown that, through careful choice of the passivating and activating polymers and/or reaction conditions, can produce NPs with tailored and desired properties.

Polymer coating materials can be classified into synthetic and natural (see Table 1). Table 1 also provides a list of synthetic and natural materials that are used to functionalize the iron oxide NPs along with their advantages, respectively. The saturation magnetization value of iron oxide NPs will decrease after polymers functionalization.

Currently, there are two major developing directions to form polymers functionalized iron oxide NPs, as follows: One is for the purpose of expanding application range by introducing the functional polymers. For instance, Gupta et al. [91] have reported a microemulsion polymerization process to prepare a poly(ethyleneglycol) (PEG)-modified superparamagnetic iron oxide NPs with magnetic core and hydrophilic polymeric shell. Highly monodispersed iron oxide NPs were synthesized by using the aqueous core of aerosol-OT (AOT)/n-Hexane reverse micelles (without microemulsions) in $N_2$ atmosphere. The average size of the PEG-modified NPs was found to be around 40–50 nm with narrow size distribution. It is important that the cytotoxicity profile of the NPs on human dermal fibroblasts as measured by standard 3-(4,5-dimethylthiazol-2-yl)-2,5-diphenyltetrazolium bromide assay showed that the particles are nontoxic and may be useful for various in vivo and in vitro biomedical applications. Another is for the purpose of manufacturing a monodisperse NPs with well-defined shape and a controlled composition. Monomer polymerization method or in-suit synthesis in the microporous of polymeric microsphere was employed for obtaining the uniform magnetic composite NPs with high content of iron oxide NPs [92]. As Zhang et al. [93] reported, an approach employs polymer microgels as templates for the synthesis

**Table 1** Organic macromolecules and their advantages of functionalized iron oxide NPs

| Polymers | | Advantages | References |
|---|---|---|---|
| Natural Polymers | Dextran | Enables optimum polar interactions with iron oxide surfaces, improves the blood circulation time, stability, and biocompatibility | [64–67] |
| | Starch | Improves the biocompatibility, good for MRI, and drug target delivery | [68, 69] |
| | Gelatin | Used as a gelling agent, hydrophilic emulsifier, biocompatible | [70–72] |
| | Chitosan | Non-toxic, alkaline, hydrophilic, widely used as non-viral gene delivery system, biocompatible, and hydrophilic | [73–75] |
| Synthetic Polymers | Poly(ethyleneglycol) (PEG) | Enhance the hydrophilicity and water-soulblility, improves the biocompatibility, blood circulation times | [76–78] |
| | Poly(vinyl alcohol) (PVA) | Prevents agglomeration, giving rise to monodispersibility | [79–81] |
| | Poly(lactide acid) (PLA) | Improves the biocompatibility, biodegradability, and low toxicity in human body | [82, 83] |
| | Alginate | Improves the stability and biocompatibility | [84, 85] |
| | Polymethylmethacrylate (PMMA) | Generally used as thermosensitive drug delivery and cell separation | [86–88] |
| | Polyacrylic acid (PAA) | Improves stability and biocompatibility as well as bioconjugation | [89, 90] |

of iron oxide NPs. At first, precursor cations were incorporated into the poly(N-isopropyl acrylamide-acrylic acid-2-hydroxyethyl acrylate) microgel particles crosslinked with N, N'-methylene bisacrylamide (BIS), then iron oxide NPs were in-suit synthesized in the microgel by co-precipitation. They show that NPs with predetermined dimensions and size-dependent properties can be synthesized by using a very delicate balance between the reaction conditions, the composition and the structure of microgel templates, and the concentration of NPs in the microgel. The synthesis of superparamagnetic $Fe_3O_4$ NPs in the microgel templates was extremely efficient: for NPs concentration as high as 0.724 g per gram polymer, the NPs had an average size of ca. 8.1 nm, low polydispersity, and showed excellent magnetic properties, while the microspheres carrying these NPs remained stimuli-responsive. Additionally, atom transfer radical polymerization (ATRP) method was utilized for obtaining monodisperse NPs with well-defined core-shell shape. ATRP can offer polymeric shells with low polydispersity and this method is easy to control the molecular weight, thereby, the thickness of the polymeric shell. Recently several polymer-coated iron oxide NPs through surface-initiated ATRP in polar solvents were successfully developed [94–97]. ATRP can be used in preparing polymers with narrow molecular weight distribution, block copolymers, graft polymers, random copolymers and finally to realize controlling the thickness of the polymeric shell and the size of polymer functionalized iron oxide NPs. As illustrated in Fig. 4, Sun et al. [98] have reported the synthesis of the iron oxide/polystyrene (PS) core/shell NPs via surface initiated ATRP. At first a method was employed to covalently bond initiators onto the surface of iron oxide NPs, which was the combination of ligands exchange reaction and condensation of triethoxysilane having an ATRP initiating site, 2-bromo-2-methyl-N-(3-(triethoxysilyl)propyl) propanamide. Then the polystyrene shell was grafted from the initiating sites on the surface of iron oxide NPs through ATRP. The covalently bonded polymeric shell could prevent the undesired site exchange of the MNPs surface functionalities. From the as-synthesized macroinitiators, the polymer functionalized iron oxide NPs with a well-defined, covalently



Fig. 4 Illustration of the synthesis route of polystyrene coated magnetic NPs with core/shell structure. From [98]
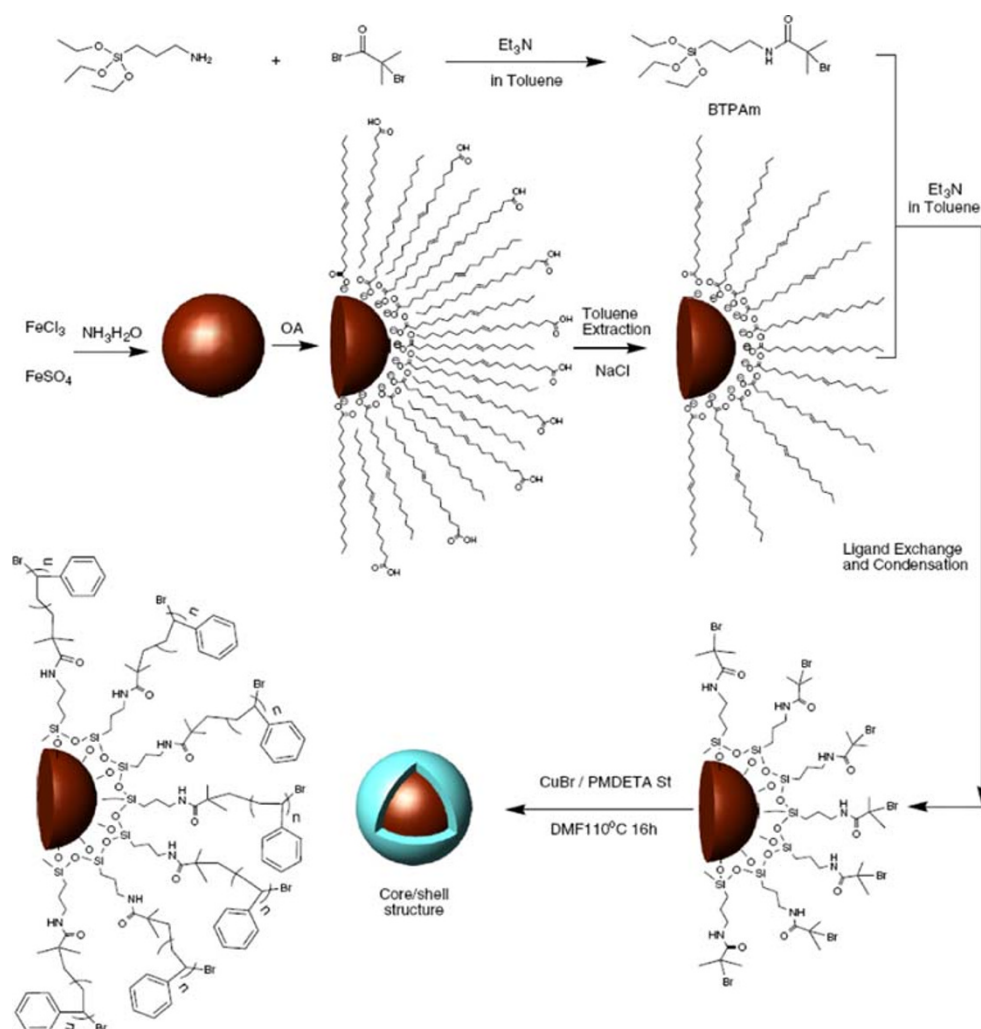
bonded PS shell have been successfully prepared through the surface initiated ATRP, which exhibits a characteristic of a controlled/"living" polymerization.

Moreover, polymer are often employed to make up the deficiency of small organic molecules and surfactant for the purpose of obtaining the surface functionalized iron oxide NPs. Therefore, besides the above research focus, how to prepare the functionalized iron oxide NPs with ideal chemical stability and good biocompatibility remains the great challenges. The right choice of organic materials can provide a structure suitable for obtaining the well-controlled functionalized NPs. For example, Frankamp et al. [99, 100] developed an approach for direct controlling the magnetic interaction between iron oxide NPs through dendrimer-mediated self-assembly. The resulting assemblies featured systematically increasing average interparticle spacing over a 2.4 nm range with increasing dendrimer generation. This increase in spacing modulated the collective magnetic behavior by effective lowering of the dipolar coupling between the particles. The dependence of blocking temperature on interparticle spacing was found to point toward a much more dramatic interdependence at close interparticle spacing, and a weaker correlation at larger spacing. Overall, the development of other methods for constructing the surface engineering of iron oxide NPs is of great important.

Biological Molecules

Various biological molecules such as protein [101, 102], polypeptide [103], antibody [104, 105], biotin and avidin [106], etc., may also be bound to the surface of iron oxide NPs directly or indirectly by chemically coupling via some functional endgroups to make the NPs target specific. The biological molecules functionalized iron oxide NPs will greatly improve the particles' biocompatibility. Such magnetic NPs can be very useful to assist an effective separation of proteins, DNA, cells, biochemical products, etc.

With appropriate surface chemistry, biomolecules can immobilize on iron oxide NPs. Zhang et al. [107] have reported a microemulsion approach to prepare a human serum albumin (HAS)-coated $Fe_3O_4$ magnetic NPs as a radioisotope carrier labeled with [188]Re and explored the optimal labeling conditions with [188]Re. The procedure for preparing HAS-coated $Fe_3O_4$ magnetic NPs as follows: With cotton oil as oil phase, a mixture of HSA and magnetite solution as water phase and Span-83 as emulsion agent. The mixture of the above two solutions was ultrasonicated for 15 min, then added rapidly dropwise into cotton oil at 130 °C under stirring condition. The diameter of HSA-coated magnetic NPs was about 200 nm. The particles can be labeled with [188]Re for the purpose of in vivo regional target therapy.

In contrast, the major strategy for surface functionalization by biological molecules includes two steps, first synthesizing the small molecules or polymers functionalized NPs, and then coupled to the biomolecules by chemical bond or physical adsorption. Recently, Lee et al. [108] developed a route for conjugating the $\gamma$-$Fe_2O_3$ NPs with single strand oligonucleotides. The water-soluble magnetic NPs with carboxyl groups on their surfaces were prepared at first, and then by using 1-ethyl-3-(3-dimrthylaminopropyl)carbodiimide hydrochloride (EDC) as a liker reagent, they successfully modified a protein, streptavidin, on the surface of $\gamma$-$Fe_2O_3$ NPs. Streptavidin functionalized $Fe_2O_3$ can catch a biotin-labeled single strand oligonucleotides through the strong affinity between streptavidin and biotin.

Additionally, superparamagnetic iron oxide core of individual NPs becomes more efficient at dephasing the spins of surrounding water protons, enhancing spin−spin relaxation times ($T_2$ relaxation times) so that the NPs act as magnetic relaxation switches (MRS) [109]. Based on this phenomenon, Perez and colleagues [110] have developed biocompatible magnetic nanosensors that act as MRS to detect molecular interactions in the reversible self-assembly of disperse magnetic particles into stable nano-assemblies recently. MRS technology can be used to detect different types of molecular interactions (DNA-DNA, protein-protein, protein-small molecule, and enzyme reactions) with high efficiency and sensitivity using magnetic relaxation measurements MRI. Furthermore, the magnetic changes are detectable in turbid media and in whole-cell lysates without protein purification. The developed magnetic nanosensors can be used in a variety of biological applications such as in homogenous assays, as reagents in miniaturized microfluidic systems, as affinity ligands for rapid and high-throughput magnetic readouts of arrays, as probes for magnetic force microscopy, and potentially for in vivo imaging. For instance, oligonucleotides functionalized iron oxide NPs aggregate in the presence of target oligonucleotides (20 pM limit), resulting in a measurable increase (30 ms) in the $T_2$ relaxation times of the surrounding water. It was further discovered that base pair insertions in the target strand resulted in only 2–5 ms increases in the relaxation times, while single base pair mismatches resulted in 1–21 ms increases in $T_2$, indicating that these systems could potentially be used to selectively detect DNA mutations.

**Surface Functionalization by Inorganic Materials**

Although there have been many significant progresses in the synthesis of organic materials functionalized iron oxide NPs, simultaneous control of their shape, stability,

biocompatibility, surface structure, and magnetic properties is still a challenge. As an alternative, inorganic compound functionalized iron oxide NPs can greatly enhance the antioxidation properties for naked iron oxide NPs, and its corresponding scope of application has been greatly extended. Moreover, inorganic compounds functionalized iron oxide NPs are very promising for application in catalysis, biolabeling, and bioseparation. The applied coating inorganic materials include silica, metal, nonmetal, metal oxides, and sulfides. Composite NPs can roughly be divided into two major parts: preserved the magnetic property of iron oxides and preserved the other properties of inorganic materials.

With controlled structure and interface interactions, nanocomposites can exhibit novel physical and chemical properties that will be essential for future technological applications. As illustrated in Fig. 5, if iron oxides were always assumed as the core, the structure of inorganic compound functionalized iron oxide NPs can roughly be divided into five types: core-shell, mosaic, shell-core, shell-core-shell, and dumbbell. Many studies have shown that in the presence of core-shell structure composite NPs, such as $Fe_3O_4$@Au NPs, its two-layer structure include magnetite core and gold shell in the outer layer. Generally, superparamagnetic colloid particles offer some attractive possibilities in bioseparation or biodetection, they should be made at dimensions they are comparable to those of a virus (20–500 nm), a protein (5–50 nm), or a DNA (10–100 nm). Nevertheless, the reactivity of iron oxide NPs has been shown to greatly increase as their dimensions are reduced, and particles with relatively small sizes may undergo rapid biodegradation when they are directly exposed to biological environments. Therefore, matrix-dispersed iron oxide NPs can be prepared in a variety of different states and greatly increase the size of naked iron oxide NPs, the three representative states have been shown in Fig. 5. The mosaic structure are commonly produced in the hollow silica spheres with iron oxide NPs, and the shell-core structure can be formed by individual iron oxides which are connected their inner layer. Additionally, $shell_a$-core-$shell_b$ type composite NPs can be obtained by layer-by-layer technology and also can be overcome the above limitations. The $shell_a$ may be the metal NPs, polymer, and quantum dots, likewise, the $shell_b$ can be the same or different functional materials. This type of

composite NPs is expected to greatly expand the application scope of iron oxide NPs. Dumbbell structure is commonly formed through epitaxial growth of iron oxide (or inorganic compound NPs) on the inorganic compound seeds (or ion oxide NPs), and finally obtained the bifunctional composite NPs.

This section, the interest arises from the possibility of combining the magnetic and the other properties by entrapping magnetic iron oxide NPs in the other inorganic compound layers, or by connecting magnetic iron oxide NPs with the other inorganic materials. We enumerate some typical and recent examples for the discussions of each feasible method and the corresponding properties and application of composite NPs.

Silica

Silica is the most common compound for preparing the functionalized iron oxide NPs, silica-coated iron oxide NPs have several advantages as follows: (a) this coating provides not only the stability to the iron oxide NPs in solution, but also avoids the interparticle interactions and prevent agglomeration generating, (b) this composite NPs possess a good biocompatibility, hydrophilicity and stability, and (c) the technology of preparation for size tunable composite NPs is already mature, and its variation of the shell thickness is relatively easy to control. In addition, silica-coating helps in binding the various biological or the other ligands at the NPs surface for various applications. For instance, Ashtari et al. [111] have reported an effective method for recovery of target ssDNA based on amino-modified silica-coated $Fe_3O_4$ NPs.

At present, the Stöber methods, sol–gel process, and aerosol pyrolysis are the prevailing choices for coating iron oxide NPs with silica. In general, silica coating will increase the size of particles and the magnetic properties of composite NPs also will change. It is noteworthy that silica thickness from 5 to 200 nm can be tuned by varying the concentration of ammonia and the ratio of tetraethoxysilane (TEOS) to water, moreover, silica coating was easily preformed on the iron oxide NPs' surface through hydroxyl groups in the aqueous environment, especially using the Stöber method and sol–gel process. This resulted in better dispersion and less aggregation of the magnetic particles. The current research focus is further extended the function

**Fig. 5** The main structure of inorganic materials functionalized iron oxide NPs (if iron oxide NPs were always assumed as the core)



Core-Shell      Mosaic      Shell-Core      Shell$_a$-Core-Shell$_b$      Dumbbell

Matrix
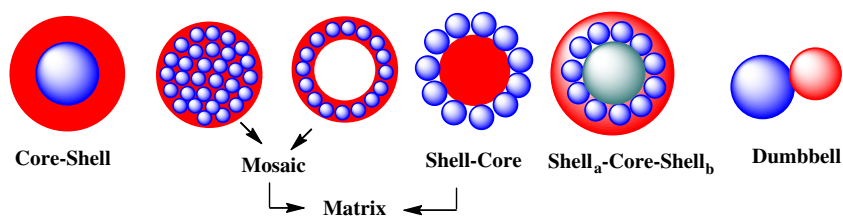
of silica functionalized iron oxide NPs, and obtains the magnetic composites with tunable structure and good dimension stability.

Therefore, for further extended function of silica functionalized iron oxide NPs, some quantum dots and other optical materials have been introduced. Ma et al. [112] reported a synthesis of $Fe_xO_y@SiO_2$ core-shell NPs by the sol–gel and modified Stöber methods. Superparamagnetic iron oxide NPs are first coated with silica to isolate the magnetic core from the surrounding. Subsequently, the dye molecules are doped inside a second silica shell based on which the dye molecules are adopted inside to improve photostability and allowed for versatile surface functionalities. The result have shown that the saturation magnetization ($M_S$) was decreased about 35 emu·g$^{-1}$ with a shell thickness of 10–15 nm after silica coating, the blocking temperature ($T_B$) and the coercivity ($H_c$) were also decreased. Yi et al. [113] have developed a pathway to synthesize magnetic quantum dots (QD) based on silica coating nanocomposite of maghemite NPs and CdSe quantum dots ($SiO_2/\gamma$-$Fe_2O_3$-CdSe, ca. 50–80 nm in size). Figure 6 shows the schematic and TEM images for synthesis of $SiO_2/\gamma$-$Fe_2O_3$-CdSe nanocomposite. The images clearly indicate the iron oxides and quantum dots with silica coating. And author claims that the presence of CdSe quantum dots increased the effective magnetic anisotropy of the $\gamma$-$Fe_2O_3$-containing NPs. The nanocomposites preserved the magnetic property of $\gamma$-$Fe_2O_3$ and optical property of CdSe quantum dots.

For obtaining the magnetic composites with tunable structure and good dimension stability still remains challenges, many skillful approaches have successfully been employed. Lu et al. [114] reported a sol–gel procedure that

leads to uniform silica-coated iron oxide NPs, and their shell thickness can be adjusted by controlling the amount of precursors (TEOS) added to the 2-propanol solution. Fluorescent dyes have also been incorporated into the silica shells by covalently coupling these organic compounds with the sol–gel precursor. These multifunctional NPs are potentially useful in a number of areas because they can be simultaneously manipulated with an externally applied magnetic field and characterized in situ using conventional fluorescence microscopy. An alternative method to prepare these NPs with uniform silica shells and tailored thickness is to use microemulsion method, also known as the water-in-oil (W/O) microemulsion process, which has three primary components: water, oil, and surfactant [115]. Homogeneous $SiO_2$-coated $Fe_2O_3$ core-shell NPs with controlled silica shell thickness from 1.8 to 30 nm had been synthesized by reverse microemulsion [116].

The aerosol pyrolysis method has recently arisen as a facile, rapid method to obtain NPs with relevant properties. Especially, by taking advantage of the subtle interplay between the parameters controlling NPs formation in aerosol process, it is possible to obtain either a continuous, three-dimensional network of particles (present a matrix structure) or a hollow structure. Moreover, aerosol pyrolysis has also been used for silica coating, but the structure of composite NPs commonly is the mosaic type, such as hollow silica spheres with iron oxide shells. Taetaj et al. [117, 118] described this method for the synthesis of superparamagnetic hollow silica spheres and the shell containing $\gamma$-$Fe_2O_3$ nanocrystals with the size range from 4 to 10 nm. The spherical composites were prepared by aerosol pyrolysis of a methanol solution containing tetraethoxysilane and iron nitrate and further annealing in a conventional
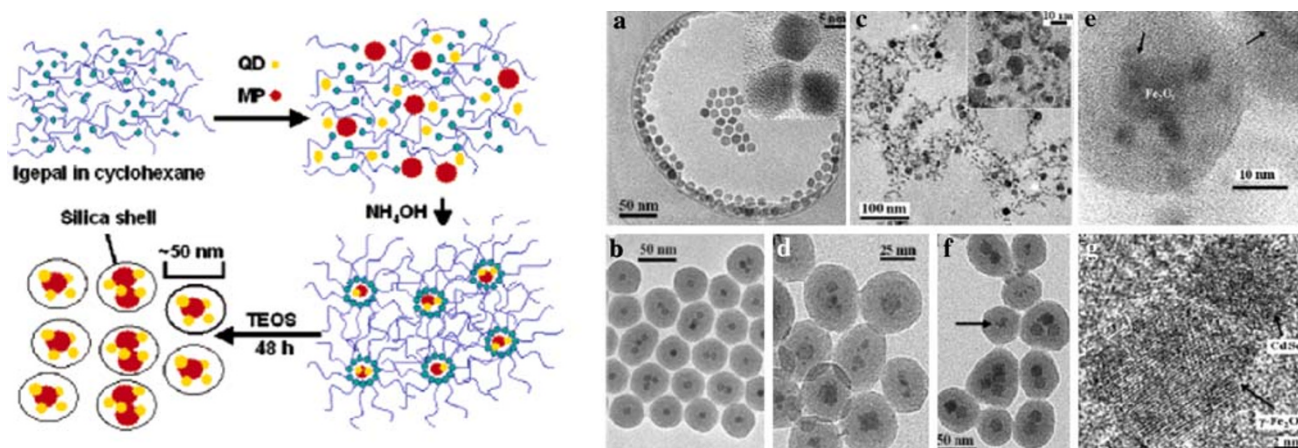


Fig. 6 Schematic for $SiO_2$/MP-QD nanocomposites synthesis (*left*); TEM micrographs of **a** $\gamma$-$Fe_2O_3$ MPs; **b** $SiO_2$/MP; **c** interconnected MPs and CdSe QDs (after 8 h of $SiO_2$/MP-QD reaction); **d**, **e** $SiO_2$/MP-QD nanocomposites (after 48 h of $SiO_2$/MP-QD reaction; note the presence of both $Fe_2O_3$ MPs and CdSe QDs (finer crystallites denoted by arrows in panel e)); and **f** $SiO_2$/MP-QD nanocomposites formed at a lower CdSe concentration (0.5 mg/mL of cyclohexane); **g** High resolution TEM micrograph of the area marked by the *arrow* in (**f**), showing the presence of CdSe QDs and $\gamma$-$Fe_2O_3$ MPs. From [113]

furnace. And it was observed that the blocking temperature ($T_B$) strongly depends on nanocomposite size, the enhancement of the effective magnetic anisotropy with respect to the bulk $\gamma$-Fe$_2$O$_3$ can be considered as coming fundamentally from surface anisotropy [119].

From the above examples, it can be seen that silica functionalized iron oxide NPs is a facile process. In this case, great progress in the field of silica-coated iron oxide NPs have been made, some research results have also being transformed into commercial application [120, 121].

Metal or Nonmetal

Another facile route to protect the iron oxide NPs is to induce a controlled oxidation of a pure single-metal or nonmetal shell, such as gold, silver, platinum, palladium, iron, carbon etc. The control of the single-metal or non-metal layer has a tremendous impact on the scope of iron oxides' application, particularly to expand its scope of biomedical and catalyst application. For instance, gold is often employed to passivate the surface of magnetite NPs to avoid oxidation. We need to notice that the gold, silver, and carbon single-metal functionalization will conduce the descend of the iron oxide NPs' saturation magnetization ($M_s$) value, but the result of cobalt, platinum, copper, palladium single-metal functionalization may be opposite, depending on the mass magnetic susceptibility ($\chi$) value of the used materials. In addition, the diameter of metallic or nonmetallic functionalized iron oxide NPs is prone to tailoring, and the necessary diameter can be obtained by controlling the reduction and repeat times.

In general, there are two ways for preparing the metal functionalized iron oxide NPs, one is direct reduction of the single-metal ions on the surface of iron oxide NPs. Mandal et al. [122] have reported that the Fe$_3$O$_4$ NPs were separated, coated with noble metal gold and silver by directly reducing the Au$^+$ and Ag$^+$, respectively, to achieve stability of the magnetic NPs for a long time, this route yielded structures of size from 18 to 30 nm, although the author claims that the NPs possess a well-defined core-shell structure, the TEM micrograph of samples cannot directly reflect. Data also showed that the saturation magnetization ($M_s$) of gold-coated is 38 emu g$^{-1}$ ($T = 10$ K) and it is reduced by 57.6% from the bulk Fe$_3$O$_4$ NPs (92 emu g$^{-1}$, $T = 10$ K). Generally, this method often applies to prepare the core-shell type composite NPs, but it is prone to maintain the magnetic properties of naked iron oxides.

On the other hand, the most common route was employed for preparing the metallic functionalized iron oxide NPs by reduction of the single-metal ion on the surface of the small molecule, polymer or SiO$_2$ functionalized iron oxide NPs. Several authors have reported the magnetic iron oxide NPs coated with gold. Gold coatings provide not only the stability to the NPs in solution, but also helps in binding the biological molecule which include -SH group at the NPs surface for various biomedical applications. Recently we [123] have adopted this approach to prepare the monodispersed gold-coated Fe$_3$O$_4$ NPs via sonolysis of a solution mixture of gold ions and amino-modified Fe$_3$O$_4$ NPs with further drop-addition of reducing agent. The composite NPs with diameter of 30 nm and their saturation magnetization ($M_s$) was 63 emu g$^{-1}$ ($T = 300$ K), and it is reduced only by ca. 0.03% from the bulk Fe$_3$O$_4$ NPs (65 emu g$^{-1}$, $T = 10$ K). Therefore, this route was beneficial to maintain the saturation magnetization ($M_s$) of the original bare magnetite NPs. Yu et al. [124] also reported a synthesis of dumbbell-like bifunctional Au-Fe$_3$O$_4$ NPs by epitaxial growth of iron oxides on the Au seeds. A mixture, consisting of Au NPs, Fe(CO)$_5$, 1-octadecene solvent, oleic acid, and oleylamine, was heated and refluxed at 300 °C followed by room temperature oxidation under air. In this way, dumbbell-like NPs were obtained with tunable sizes in the range 3–14 nm. As illustrated in Fig. 7, Stoeva et al. [125] skillfully used shell-core type functionalized iron oxide NPs (SiO$_2$/Fe$_3$O$_4$ NPs) that electrostatically attract 1–3 nm gold-nanoparticle seeds which act in a subsequent step as nucleation sites for the formation of a continuous gold shell around the shell-core NPs upon HAuCl$_4$ reduction. The author also demonstrates that these three-layer magnetic NPs can be functionalized with DNA following synthetic methods for pure gold NPs and reversibly assembled into macroscopic aggregates using complementary linking oligonucleotides. Additionally, Teng et al. [126] have reported a one-pot sequential synthetic method for the synthesis of well-defined and shell-thickness-tunable Pt@Fe$_2$O$_3$ core-shell NPs. These Pt@Fe$_2$O$_3$ core-shell NPs could have potential applications in catalysis and as precursors for making property-tunable magnetic NPs, thin films, and nanocomposites.

Taking into account the application prospects of magnetic record and magnetic ink materials recently, most studies have focused on the development of carbon-coated iron oxide magnetic NPs (such as carbon-encapsulated magnetic NPs), the carbon shell not only protected the iron oxide NPs from rapidly degraded by environment, but it also prevented the NPs' agglomeration caused by *van der Waals* attraction. Though carbon-coated will cause the reduction of saturation magnetization, the other magnetic properties will change little. Moreover, carbon functionalized iron oxide NPs have many advantages over the other materials, such as much higher chemical and thermal stability as well as biocompatibility. Recent methods offer new alternatives for the controlled synthesis of novel, stable, and functional iron oxides/C NPs. Wang et al. [127] reported the preparation of Fe$_3$O$_4$/C nanocomposition by heating the aqueous solution of glucose and oleic
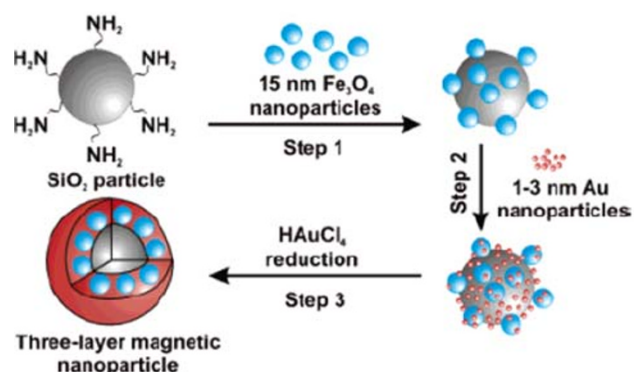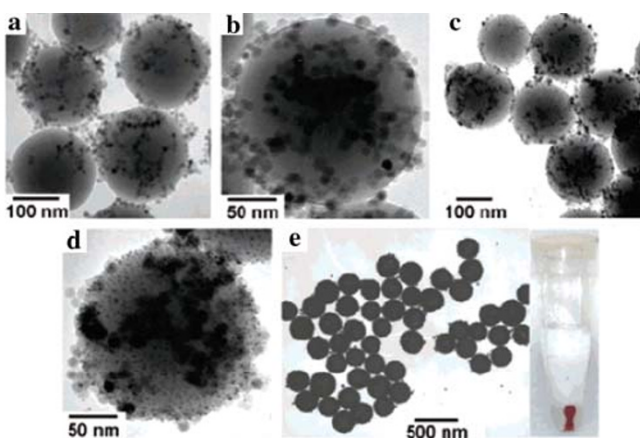
**Fig. 7** Synthetic scheme for the preparation of the three-layer NPs (*left*); TEM images of colloids after each synthetic step. **a**, **b** SiO$_2$ particles covered with silica-primed Fe$_3$O$_4$ NPs (SiO$_2$–Fe$_3$O$_4$). **c**, **d** SiO$_2$ particles covered with silica-primed Fe$_3$O$_4$ NPs and heavily loaded with Au nanoparticle seeds (SiO$_2$–Fe$_3$O$_4$–Au seeds). **e** Three-

layer magnetic NPs synthesized in a single-step process from particles presented in (**c**) and (**d**). Note the uniformity of the gold shell. The inset shows the three-layer magnetic NPs drawn to the wall with a magnet. From [125]

acid-stabilized magnetite NPs. Dantas et al. [128] reported the synthesis of iron oxides/C composites, and it can be used in the treatment of textile waste water as heterogeneous catalysts in the Fenton reaction. Though carbon-coated iron oxide NPs have many advantageous properties, the synthesis of monodispersed composite NPs in isolated from is currency one of challenges in this field.

Furthermore, single-metal functionalized iron oxide NPs (especially noble metal functionalized iron oxide NPs, and mostly take the direct method by reducing the single-metal ions on the surface of iron oxide NPs) also used as catalysts, such as Au/Fe$_2$O$_3$ catalyst for CO oxidation [129, 130], Au/α-Fe$_2$O$_3$ catalyst for water-gas shift reaction [131, 132], Fe$_3$O$_4$/Pd nanoparticle-based catalyst for the cross-coupling of acrylic acid with iodobenzene [133] and de-carboxylative coupling reaction in aqueous media [134], Ag-Fe$_3$O$_4$ catalyst for epoxidation of styrene [135], etc. These heterogeneous catalysts with a matrix structure generally as the magnetically recyclable catalysts (MRCs) are developed in recent years and can be very useful to

assist an effective separation and recovery in a liquid-phase reaction by a magnet, especially when the catalysts are in the nanometer-sized range and possess higher activities than their pure and bulk single-metal or nonmetal counterparts [136, 137]. Therefore, the development of the facile and rapid methods for the preparation of efficient MRCs is still a challenge.

Hence, many efforts have been made for getting the nanometer-sized MRCs with high activity and easy separation properties. For example, a Au/Fe$_x$O$_y$ catalyst with high CO oxidation activities at low temperature prepared by deposition–precipitation (DP) method was reported by Lin and Chen [138]. In this work, the size and surface area of MRCs can be adjusted by the PH value during the DP process and the calcination temperature. Moreover, after 90 min time on stream, the conversion of CO can be reached 100%. Additionally, a comparative study results by Avgouropoulos et al. [139] shows that the Au/α-Fe$_2$O$_3$ catalyst is superior to the Pt/γ-Al$_2$O$_3$ and Cuo-CeO$_2$ for the selective CO oxidation at relatively low reaction

**Fig. 8** Illustration of the preparation of Fe$_3$O$_4$@SiO$_2$–Gn–PAMAM–Pd(0) inorganic–organic hybrid composites (*left*); HRTEM images of MRCs (*Right*). From [140]
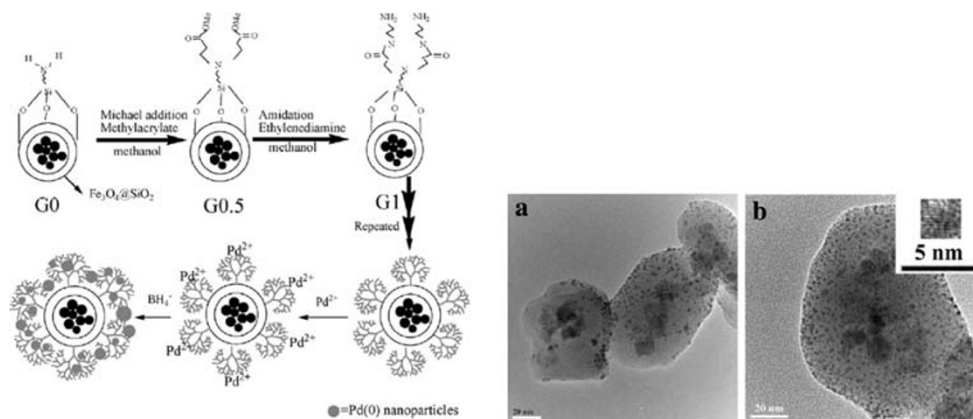
temperatures (<80–120 °C, depending on contact time and feed composition employed). As illustrated in Fig. 8, Jiang et al. [140] have reported a indirect route for preparing the $Fe_3O_4@SiO_2$-Gn-PAMAM-Pd(0) matrixs composites ($n = 0$–4, where $n$ is the generation of the dendrimer, abbreviated as Gn, the MRCs possess a high conversion >99.5%) and their applications as MRCs for the hydrogenation of allyl alcohol. Pd NPs with diameters of about 2.5 nm were stabilized homogeneously on the surface of $Fe_3O_4@SiO_2$-Gn-PAMAM and the sizes of the magnetic composite NPs are about 60–100 nm. These characteristics of the systems lead to the high catalytic activity for hydrogenation of allyl alcohol, and the rate of the reaction can also be controlled by changing the generation of PAMAM. The silica in the system may physically protect the $Fe_3O_4$ core apart from corruption in the reaction environments and the surface functional groups may contact PAMAM tightly.

## Metal Oxides/Sulfides

There have been abundant researches concerning the metal oxides or metal sulfides functionalized iron oxide NPs, mainly because of its importance of unique physical or chemical properties. In general, researches primarily concentrate on common materials ($ZnO$, $MgO$, $CaO$, $SnO_2$, $Al_2O_3$ etc.) [141–144], magnetic materials (iron oxides, $CoO$, $NiO$, $CoFe_2O_4$, etc.) [145], optical and electrical functional materials ($TiO_2$, $ZnS$, $Y_2O_3$, etc.) [146–148].

Recently common materials coated on the surface of iron oxide NPs are receiving more attention, because it usually imports metal oxides' special properties. Li et al. [149] reported a chemical displacement procedure that leads to air-stable $Fe_3O_4@Al_2O_3$ core-shell NPs. The NPs are rather uniform and they claim that it with captured phosphopeptides were directly deposited on the MALDI (matrix-assisted laser desorption/ionization) target for analysis due to its high magnetic response. Hong et al. [150] reported ZnO-coated magnetite core-shell NPs were obtained by coating the $Fe_3O_4$ NPs with direct precipitation using zinc acetate and ammonium carbonate. They claim that the functionalized NPs' antioxidation ability is much better than the naked $Fe_3O_4$ NPs. However, the particles obtained are not very uniform and its saturation magnetization ($M_s$) decrease from 67.78 to 20.33 emu/g.

Magnetic materials coated on the iron oxide NPs usually have a dramatic influence on the magnetic properties. The combination of two different magnetic phases will lead to new functionalized iron oxide NPs, with many possible applications. Cheon et al. [6, 151] reported the fabrication of highly ordered binary $Fe_3O_4@CoFe_2O_4$ NPs by superlattices transition; the preparation process shows a unique ferrimagnetic phase transformation behavior through nanoscale redox chemical reactions, the particles'
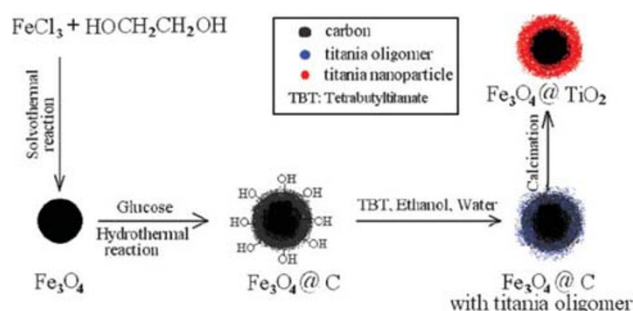


**Fig. 9** Scheme of the synthetic route to $Fe_3O_4@TiO_2$ core-shell NPs. From [153]

saturation magnetization have been greatly enhanced, and its coercivity ($H_C$) increased from 580 to 15,000 Oe.

In addition, optical and electrical materials functionalized iron oxide NPs obviously enable the enlargement of the iron oxide NPs' application scope. For example, Wang et al. introduced the superparamagnetic $\gamma$-$Fe_2O_3$ beads-CdSe@ZnS quantum dots NPs prepared by thiol–metal bonds conjunction, and their average diameter of this luminescent/magnetic nanocomposite was ca. 20 nm, and it exhibited high emission quantum yield and, was easily separated from solution by magnetic decantation using a permanent magnet. The NPs were used in cell separation and would be used in a variety of bioanalytical assays involving luminescence detection and magnetic separation [152]. Recently Li et al. [153] reported a synthesis of $Fe_3O_4@TiO_2$ composite NPs by a indirect route that involves three steps (Fig. 9). First, magnetite NPs were synthesized via a solvothermal reaction, using $FeCl_3$ as the source of magnetite, and ethylene glycol as both the solvent and reductant. Then, the magnetite NPs were coated with a thin layer of carbon by the polymerization and carbonization of glucose through a hydrothermal reaction, resulting in $Fe_3O_4@C$ NPs. Finally, tetrabutyltitanate was pre-hydrolyzed and absorbed onto the composite NPs, and eventually converted into titania by calcination under nitrogen. Moreover, this composite NPs can be used for selective enrichment of phosphopeptides easily in phosphoproteome analysis as it possesses the magnetic properties [154]. In addition, Chen et al. [155] have reported the functional $Fe_3O_4/TiO_2$ core/shell magnetic NPs can be as photokilling agents for pathogenic bacteria. Therefore, more and more optical and electrical materials functionalized materials functionalized iron oxide NPs have been employed for the biological technology.

## Conclusions and Future Outlook

Although in this review there are various strategies for obtaining the functionalized iron oxide NPs, the results have shown that three major effectivenesses as follows:

(a) Improves the biocompatibility and chemical stability, and tailors the dispersibility and water solubility; (b) Endows the iron oxide new physico-chemical properties, such as magnet-optical properties, magnetic-electrical properties, magnetic-thermal properties, etc.; (c) Provides the iron oxide new functional endgroups for the subsequent functionalized procedures or the subsequent applications, such as conjugation with the DNA, antibody, protein, etc.

In the coming years, despite all the recent progresses made, it is still a challenge to be faced that synthesis of high-quality functionalized magnetic iron oxide NPs with a tunable sizes and shapes in a controlled manner. Moreover, synthesis and surface engineering of iron oxide NPs involves complex chemical, physical, and physicochemical multiple interactions, it is the another challenge to understand the synthetic mechanisms detailedly. However, the magnetic properties and function of naked or surface functionalized iron oxide NPs depend upon their physical properties: the size and shape, their microstructure, and the chemical phase in which they are present [156]. Luckily, several physicochemical techniques have been developed to determine these parameters.

Therefore, how to improve the stability and availability of functionalized iron oxide NPs in extreme environmental conditions, how to develop an efficient and orderly magnetic micro- or nano-assembly structures, and how to realize large-scale or industrial synthesis, these problems are urgent to be solved for obtaining a ideal functionalized iron oxide materials.

For all that, we still believe the surface functionalization and modification of magnetic iron oxide NPs to introduce additional functionality will attract more and more attention. Furthermore, multifunctional magnetic iron oxide composite nanoparticle systems with designed active sites will promise for a various applications, such as catalysts, magnetic recording, bioseparation, biodetection, etc. The future work in this area must be focused on the research of the toxicity and degradability of naked or surface functionalized iron oxide NPs, and preparing it via green chemistry for reducing the environmental pollution as much as possible. Successful development in this area will aid the growth of the various scientific researches or industrial applications as well as improving the quality of life in the population.

## References

1. L. LaConte, N. Nitin, G. Bao, Mater. Today **8**, 32 (2005). doi:10.1016/S1369-7021(05)00893-X

2. D. Patel, J.Y. Moon, Y. Chang, T.J. Kim, G.H. Lee, Colloid Surf. A **313–314**, 91 (2008). doi:10.1016/j.colsurfa.2007.04.078

3. M. Zhao, L. Josephson, Y. Tang, R. Weissleder, Angew. Chem. Int. Ed. **42**, 1375 (2003). doi:10.1002/anie.200390352

4. S. Mornet, S. Vasseur, F. Grasset, P. Veverka, G. Goglio, A. Demourgues et al., Prog. Solid State Chem. **34**, 237 (2006). doi:10.1016/j.progsolidstchem.2005.11.010

5. P.D. Stevens, J. Fan, H.M.R. Gardimalla, M. Yen, Y. Gao, Org. Lett. **7**, 2085 (2005). doi:10.1021/ol050218w

6. Y. Jun, J. Choi, J. Cheon. Chem. Commun. (Camb) 1203 (2007). doi:10.1039/b614735f

7. A.K. Gupta, M. Gupta, Biomaterials **26**, 3995 (2005). doi:10.1016/j.biomaterials.2004.10.012

8. R.M. Cornell, U. Schwertmann, *The Iron Oxides: Structures, Properties, Reactions, Occurences and Uses* (Wiley-VCH, Weinheim, 2003)

9. L. Cabrera, S. Gutierrez, N. Menendezb, M.P. Morales, P. Herrasti, Electrochim. Acta **53**, 3436 (2008)

10. C. Pascal, J.L. Pascal, F. Favier, M.L.E. Moubtassim, C. Payen, Chem. Mater. **11**, 141 (1999). doi:10.1021/cm980742f

11. O. Bomatí-Miguel, L. Mazeina, A. Navrotsky, S. Veintemillas-Verdaguer, Chem. Mater. **20**, 591 (2008). doi:10.1021/cm071178o

12. A.A. Bharde, R.Y. Parikh, M. Baidakova, S. Jouen, B. Hannoyer, T. Enoki et al., Langmuir **24**, 5787 (2008). doi:10.1021/la704019p

13. Y. Roh, H. Vali, T.J. Phelps, J.W. Moon, J. Nanosci. Nanotechnol. **11**, 3517 (2006)

14. W. Wu, Q. He, R. Hu, J. Huang, H. Chen, Rare Metal Mater. Eng. **34**, 238 (2007)

15. V.J. Binh, S.T. Purcell, V. Semet, F. Feschet, Appl. Surf. Sci. **130–132**, 803 (1998). doi:10.1016/S0169-4332(98)00158-5

16. Y.S. Kang, S. Risbud, J.F. Rabolt, P. Stroeve, Chem. Mater. **8**, 2209 (1996). doi:10.1021/cm960157j

17. A.A. Novakova, V.Y. Lanchinskaya, A.V. Volkov, T.S. Gendler, T.Y. Kiseleva, M.A. Moskvina et al., J. Magn. Magn. Mater. **258–259**, 35 (2003). doi:10.1016/S0304-8853(02)01062-4

18. J. Lee, T. Isobe, M. Senna, Colloids Surf. A Physicochem. Eng. Asp. **109**, 121 (1996). doi:10.1016/0927-7757(95)03479-X

19. S. Sun, H. Zeng, J. Am. Chem. Soc. **124**, 8204 (2002). doi:10.1021/ja026501x

20. J. Rockenberger, E.C. Scher, P.A. Alivisatos, J. Am. Chem. Soc. **121**, 11595 (1999). doi:10.1021/ja993280v

21. K. Woo, J. Hong, S. Choi, H. Lee, J. Ahn, C.S. Kim et al., Chem. Mater. **16**, 2814 (2004). doi:10.1021/cm049552x

22. T. Hyeon, S.S. Lee, J. Park, Y. Chung, H.B. Na, J. Am. Chem. Soc. **123**, 12798 (2001). doi:10.1021/ja016812s

23. C. Solans, P. Izquierdo, J. Nolla, N. Azemar, M.J. Garcia-Celma, Curr. Opin. Colloid Interface Sci. **10**, 102 (2005). doi:10.1016/j.cocis.2005.06.004

24. J. Vidal-Vidal, J. Rivas, M.A. López-Quintela, Colloid Surf. A **288**, 44 (2006). doi:10.1016/j.colsurfa.2006.04.027

25. F.A. Tourinho, R. Franck, R. Massart, J. Mater. Sci. **25**, 3249 (1990). doi:10.1007/BF00587682

26. A.B. Chin, I.I. Yaacob, J. Mater. Process. Technol. **191**, 235 (2007). doi:10.1016/j.jmatprotec.2007.03.011

27. X. Hu, J.C. Yu, J. Gong, J. Phys. Chem. C **111**, 11180 (2007). doi:10.1021/jp073073e

28. S. Giria, S. Samantab, S. Majic, S. Gangulic, A. Bhaumikb, J. Magn. Magn. Mater. **285**, 296 (2005). doi:10.1016/j.jmmm.2004.08.007

29. Z. Jing, S. Wu, Mater. Lett. **58**, 3637 (2004). doi:10.1016/j.matlet.2004.07.010

30. X. Liu, G. Qiu, A. Yan, Z. Wang, X. Li, J. Alloy Compd. **433**, 216 (2007). doi:10.1093/comjnl/bxm059

31. J. Wang, J. Sun, Q. Sun, Q. Chen, Mater. Res. Bull. **38**, 1113 (2003). doi:10.1016/S0025-5408(03)00129-6
32. Y. Zheng, Y. Cheng, F. Bao, Y. Wang, Mater. Res. Bull. **41**, 525 (2006). doi:10.1016/j.materresbull.2005.09.015
33. T.J. Daou, G. Pourroy, S. Bégin-Colin, J.M. Grenéche, C. Ulhaq-Bouillet, P. Legaré et al., Chem. Mater. **18**, 4399 (2006). doi:10.1021/cm060805r
34. S. Wang, Y. Min, S. Yu, J. Phys. Chem. C **111**, 3551 (2007). doi:10.1021/jp068647e
35. M.M. Titirici, M. Antonietti, A. Thomas, Chem. Mater. **18**, 3808 (2006). doi:10.1021/cm052768u
36. K.S. Suslick, Science **247**, 1439 (1990). doi:10.1126/science.247.4949.1439
37. J.H. Bang, K.S. Suslick, J. Am. Chem. Soc. **129**, 2242 (2007). doi:10.1021/ja0676657
38. R. Vijayakumar, Y. Koltypin, I. Felner, A. Gedanken, Mater. Sci. Eng. A **286**, 101 (2000). doi:10.1016/S0921-5093(00)00647-X
39. J. Pinkas, V. Reichlova, R. Zboril, Z. Moravec, P. Bezdicka, J. Matejkova, Ultrason. Sonochem. **15**, 257 (2008). doi:10.1016/j.ultsonch.2007.03.009
40. P.C. Scholten, *Thermodynamics of Magnetic Fluids* (Hemisphere, Washington, DC, 1978)
41. R.E. Rosensweig, R. Kaiser, G. Miskolszy, J. Colloid Interface Sci. **29**, 680 (1969). doi:10.1016/0021-9797(69)90220-3
42. R. Tadmor, R.E. Rosensweig, J. Frey, J. Klein, Langmuir **16**, 9117 (2000). doi:10.1021/la0009137
43. Y. Sahoo, A. Goodarzi, M.T. Swihart, T.Y. Ohulchanskyy, E.P. Furlani, P.N. Prasad, J. Phys. Chem. B **109**, 3879 (2005). doi:10.1021/jp045402y
44. A.B. Bourlinos, A. Simopoulos, D. Petridis, Chem. Mater. **14**, 899 (2002). doi:10.1021/cm010794w
45. M.H. Sousa, J.C. Rubim, P.G. Sobrinho, F.A. Tourinho, J. Magn. Magn. Mater. **225**, 67 (2001). doi:10.1016/S0304-8853(00)01229-4
46. P.C. Morais, A.C. Oliveira, A.L. Tronconi, T. Goetze, N. Buske, IEEE Trans. Magn. **39**, 2654 (2003). doi:10.1109/TMAG.2003.815544
47. S. Mornet, S. Vasseur, F. Grasset, E. Duguet, J. Mater. Chem. **14**, 2161 (2004). doi:10.1039/b402025a
48. J. Xie, C.H. Wang, Pharm. Res. **22**, 2079 (2005). doi:10.1007/s11095-005-7782-y
49. S.S. Banerjee, D. Chen, Chem. Mater. **19**, 6345 (2007). doi:10.1021/cm702278u
50. Y. Hou, H. Kondoh, M. Shimojo, E.O. Sako, N. Ozaki, T. Kogure et al., J. Phys. Chem. B **109**, 4845 (2005). doi:10.1021/jp0476646
51. D. Bonacchi, A. Caneschi, D. Dorignac, A. Falqui, D. Gatteschi, D. Rovai et al., Chem. Mater. **16**, 2016 (2004). doi:10.1021/cm034948e
52. H. Xia, J. Yi, P. Foo, B. Liu, Chem. Mater. **19**, 4087 (2007). doi:10.1021/cm070918q
53. Z.P. Chen, Y. Zhang, S. Zhang, J.G. Xia, J.W. Liu, K. Xu et al., Colloid Surf. A **316**, 210 (2008). doi:10.1016/j.colsurfa.2007.09.017
54. R.S. Ingram, M.J. Hostetler, R.W. Murray, J. Am. Chem. Soc. **119**, 9175 (1997). doi:10.1021/ja971734n
55. M.J. Hostetler, S.J. Green, J.J. Stokes, R.W. Murray, J. Am. Chem. Soc. **118**, 4212 (1996). doi:10.1021/ja960198g
56. S. Sun, H. Zeng, D.B. Robinson, S. Raoux, P.M. Rice, S.X. Wang et al., J. Am. Chem. Soc. **126**, 273 (2004). doi:10.1021/ja0380852
57. M. Lattuada, T.A. Hatton, Langmuir **23**, 2158 (2007). doi:10.1021/la062092x
58. J. Fan, J. Lu, R. Xu, R. Jiang, Y. Gao, J. Colloid Interface Sci. **266**, 215 (2003). doi:10.1016/S0021-9797(03)00570-8
59. X. Shen, X. Fang, Y. Zhou, H. Liang, Chem. Lett. **33**, 1468 (2004). doi:10.1246/cl.2004.1468
60. M. Ma, Y. Zhang, W. Yu, H. Shen, H. Zhang, N. Gu, Colloid Surf. A **212**, 219 (2003). doi:10.1016/S0927-7757(02)00305-9
61. B. Arales, Chemtechnology **7**, 766 (1977)
62. W. Wu, Q. He, H. Chen, in *Proceedings of the 1st International Conference on Bioinformatics and Biomedical Engineering (Wuhan)*, vol. 1, 2007, pp. 76
63. R.D. Palma, S. Peeters, M.J. Van Bael, H. Van den Rul, K. Bonroy, W. Laureyn et al., Chem. Mater. **19**, 1821 (2007). doi:10.1021/cm0628000
64. C.C. Berry, A.S.G. Curtis, J. Phys, D. Appl. Phys. (Berl) **36**, R198 (2003)
65. C.C. Berry, S. Wells, S. Charles, A.S.G. Curtis, Biomaterials **24**, 4551 (2003). doi:10.1016/S0142-9612(03)00237-0
66. M. Mikhaylova, D.K. Kim, N. Bobrysheva, M. Osmolowsky, V. Semenov, T. Tsakalakos et al., Langmuir **20**, 2472 (2004). doi:10.1021/la035648e
67. M.C. Bautista, O. Bomati-Miguel, M.P. Morales, C.J. Serna, S. Veintemillas-Verdaguer, J. Magn. Magn. Mater. **293**, 20 (2005). doi:10.1016/j.jmmm.2005.01.038
68. D.K. Kim, M. Maria, F.H. Wang, K. Jan, B. Börje, Y. Zhang et al., Chem. Mater. **15**, 4343 (2003). doi:10.1021/cm031104m
69. W. Wang, Z.K. Zhang, J. Disper, Sci. Technol. **28**, 557 (2007)
70. D. Olsena, C. Yanga, M. Bodoa, R. Changa, S. Leigha, J. Baeza et al., Adv. Drug. Deliv. Rev. **55**, 1547 (2003). doi:10.1016/j.addr.2003.08.008
71. B. Gaihre, S. Aryal, M.S. Khil, H.Y. Kim, J. Microencapsul. **25**, 21 (2008). doi:10.1080/02652040701737697
72. T. Yonezawa, K. Kamoshita, M. Tanaka, T. Kinoshita, Jpn. J. Appl. Phys. **47**, 1389 (2008). doi:10.1143/JJAP.47.1389
73. G. Li, K. Huang, Y. Jiang, P. Ding, D. Yang, Biochem. Eng. J. (2008). doi:10.1016/j.bej.2008.01.018
74. G. Li, Y. Jiang, K. Huang, P. Ding, L. Yao, Colloid. Surf. A (2008). doi:10.1016/j.colsurfa.2008.01.017
75. E.H. Kim, H.S. Lee, B.K. Kwak, B.K. Kim, J. Magn. Magn. Mater. **289**, 328 (2005). doi:10.1016/j.jmmm.2004.11.093
76. S. Mondini, S. Cenedese, G. Marinoni, G. Molteni, N. Santo, C.L. Bianchi et al., J. Colloid Interface Sci. **322**, 173 (2008). doi:10.1016/j.jcis.2008.03.008
77. K.G. Paul, T.B. Frigo, J.Y. Groman, E.V. Groman, Bioconjug. Chem. **15**, 394 (2004). doi:10.1021/bc034194u
78. S.M. Moghimi, A.C. Hunter, J.C. Murray, Pharmacol. Rev. **53**, 283 (2001)
79. H. Pardoe, W. Chua-anusorn, T.G. Pierre, J. Dobson, J. Magn. Magn. Mater. **225**, 41 (2001). doi:10.1016/S0304-8853(00)01226-9
80. M. Chastellain, A. Petri, H.J. Hofmann, Colloid Interface Sci. **278**, 353 (2004). doi:10.1016/j.jcis.2004.06.025
81. A.J.M. D'Souza, R.L. Schowen, E.M. Topp, J Control Release **94**, 91 (2004). doi:10.1016/j.jconrel.2003.09.014
82. F. Chen, Q. Gao, G. Hong, J. Ni, J. Magn. Magn. Mater. **320**, 1921 (2008). doi:10.1016/j.jmmm.2008.02.132
83. S.A. Gomez-Lopera, J.L. Arias, V. Gallardo, A.V. Delgado, Langmuir **22**, 2816 (2006). doi:10.1021/la0530079
84. H.L. Ma, Y.F. Xu, X.R. Qi, Y. Maitani, T. Nagai, Int. J. Pharm. **354**, 217 (2006). doi:10.1016/j.ijpharm.2007.11.036
85. M.A. Morales, P.V. Finotelli, J.A.H. Coaquira, M.H.M. Rocha-Leão, C. Diaz-Aguila, E.M. Baggio-Saitovitch et al., Mater. Sci. Eng. C **28**, 253 (2007). doi:10.1016/j.msec.2006.12.016
86. D.M. Zhu, F. Wang, M. Han, H.B. Li, Z. Xu, Chin. J. Inorg. Chem. **23**, 2128 (2007)
87. H. Singh, P.E. Laibinis, T.A. Hatton, Langmuir **21**, 11500 (2005). doi:10.1021/la0517843
88. L. An, Z. Li, Y. Wang, B. Yang, Chem. J. Chin. Univ. **27**, 1372 (2006)

89. G. Shan, J. Xing, M. Luo, H. Liu, J. Chen, Biotechnol. Lett. **25**, 1977 (2003). doi:10.1023/B:BILE.0000004388.15751.8c

90. A.S. Arbab, L.A. Bashaw, B.R. Miller, E.K. Jordan, B.K. Lewis, H. Kalish et al., Radiology **229**, 838 (2003). doi:10.1148/radiol.2293021215

91. A.K. Gupta, S. Wells, IEEE Trans. Nanobioscience **3**, 66 (2004). doi:10.1109/TNB.2003.820277

92. D. Guin, S.V. Manorama, Mater. Lett. **62**, 3139 (2008). doi:10.1016/j.matlet.2008.02.005

93. J. Zhang, S. Xu, E. Kumacheva, J. Am. Chem. Soc. **126**, 7908 (2004). doi:10.1021/ja031523k

94. T. Ninjbadgar, S. Yamamoto, T. Fukuda, Solid State Sci. **6**, 879 (2004). doi:10.1016/j.solidstatesciences.2003.11.009

95. Q. Fan, K. Neoh, E. Kang, B. Shuter, S. Wang, Biomaterials **28**, 5426 (2007). doi:10.1016/j.biomaterials.2007.08.039

96. Y. Zhou, S. Wang, B. Ding, Z. Yang, Chem. Eng. J. **138**, 578 (2008). doi:10.1016/j.cej.2007.07.030

97. E. Marutani, S. Yamamoto, T. Ninjbadgar, Y. Tsujii, T. Fukuda, M. Takano, Polymer (Guildf) 45:2231 (2004). doi:10.1016/j.polymer.2004.02.005

98. Y. Sun, X. Ding, Z. Zheng, X. Cheng, X. Hu, Y. Peng, Eur. Polym. J. **43**, 762 (2007). doi:10.1016/j.eurpolymj.2006.10.021

99. B.L. Frankamp, A.K. Boal, M.T. Tuominen, V.M. Rotello, J. Am. Chem. Soc. **127**, 9731 (2005). doi:10.1021/ja051351m

100. A.K. Boal, K. Das, M. Gray, V.M. Rotello, Chem. Mater. **14**, 2628 (2002). doi:10.1021/cm011689p

101. H. He, H. Liu, K. Zhou, W. Wang, P. Rong, J. Cent. South Univ. Technol. **13**, 6 (2006). doi:10.1007/s11771-006-0097-2

102. M. Mikhaylova, D.K. Kim, C.C. Berry, A. Zagorodni, M. Toprak, A.S.G. Curtis et al., Chem. Mater. **16**, 2344 (2004). doi:10.1021/cm0348904

103. M. Lewin, N. Carlesso, C. Tung, X. Tang, D. Cory, D.T. Scadden et al., Nat. Biotechnol. **18**, 410 (2000). doi:10.1038/74464

104. L.X. Tiefenauer, G. Kuhne, R.Y. Andres, Bioconjug. Chem. **4**, 347 (1993). doi:10.1021/bc00023a007

105. J.M. Nam, S.I. Stoeva, C.A. Mirkin, J. Am. Chem. Soc. **126**, 5932 (2004). doi:10.1021/ja049384+

106. Y. Weizmann, F. Patolsky, O. Lioubashevski, I. Willner, J. Am. Chem. Soc. **126**, 1073 (2004). doi:10.1021/ja038257v

107. C. Zhang, J. Cao, D. Yin, Y. Wang, Y. Feng, J. Tan, Appl. Radiat. Isot. **61**, 1255 (2004). doi:10.1016/j.apradiso.2004.03.114

108. C. Lee, K. Huang, P. Wei, Y. Yao, J. Magn. Magn. Mater. **304**, e412 (2006). doi:10.1016/j.jmmm.2006.01.213

109. L. Josephson, J.M. Perez, R. Weissleder, Angew. Chem. Int. Ed. **40**, 3204 (2001). doi:10.1002/1521-3773(20010903)40:17<3204::AID-ANIE3204>3.0.CO;2-H

110. N.L. Rosi, C.A. Mirkin, Chem. Rev. **105**, 1547 (2005). doi:10.1021/cr030067f

111. P. Ashtari, X. He, K. Wang, P. Gong, Talanta **67**, 548 (2005). doi:10.1016/j.talanta.2005.06.043

112. D. Ma, J. Guan, F. Normandin, S. Dénommée, G. Enright, T. Veres et al., Chem. Mater. **18**, 1920 (2006). doi:10.1021/cm052067x

113. D.K. Yi, S.T. Selvan, S.S. Lee, G.C. Papaefthymiou, D. Kundaliya, J.Y. Ying, J. Am. Chem. Soc. **127**, 4990 (2005). doi:10.1021/ja0428863

114. Y. Lu, Y. Yin, B.T. Mayers, Y. Xia, Nano. Lett. **2**, 183 (2002). doi:10.1021/nl015681q

115. J.E. Smith, L. Wang, W. Tan, Trends Analyt. Chem. **25**, 848 (2006). doi:10.1016/j.trac.2006.03.008

116. D.K. Yi, S.S. Lee, G.C. Papaefthymiou, Chem. Mater. **3**, 604 (2006)

117. P. Tartaj, T. Gonzalez-Carreno, C.J. Serna, Adv. Mater. **13**, 1620 (2001). doi:10.1002/1521-4095(200111)13:21<1620::AID-ADMA1620>3.0.CO;2-Z

118. P. Tartaj, T. Gonzalez-Carreno, C.J. Serna, Adv. Mater. **16**, 529 (2004). doi:10.1002/adma.200305814

119. P. Tartaj, T. Gonzalez-Carreno, C.J. Serna, J. Phys. B **107**, 20 (2003)

120. I.J. Brucea, J. Taylor, M. Todd, M.J. Daviesb, E. Borionib, C. Sangregorioa et al., J. Magn. Magn. Mater. **284**, 145 (2004). doi:10.1016/j.jmmm.2004.06.032

121. V. Salgueirino-Maceira, M.A. Correa-Duarte, M. Spasova, L.M. Liz-Marzan, M. Farle, Adv. Funct. Mater. **16**, 509 (2006). doi:10.1002/adfm.200500565

122. M. Mandal, S. Kundu, S.K. Ghosh, S. Panigrahi, T.K. Sau, J. Colloid Interface Sci. **286**, 187 (2005). doi:10.1016/j.jcis.2005.01.013

123. W. Wu, Q. He, H. Chen, J. Tang, L. Nie, Nanotechnology **18**, 145609 (2007). doi:10.1088/0957-4484/18/14/145609

124. H. Yu, M. Chen, P.M. Rice, S.X. Wang, R.L. White, S. Sun, Nano. Lett. **5**, 379 (2005). doi:10.1021/nl047955q

125. S.I. Stoeva, F. Huo, J.S. Lee, C.A. Mirkin, J. Am. Chem. Soc. **127**, 15362 (2005). doi:10.1021/ja055056d

126. X. Teng, D. Black, N.J. Watkins, Y. Gao, H. Yang, Nano. Lett. **3**, 261 (2003). doi:10.1021/nl025918y

127. Z. Wang, H. Guo, Y. Yu, N. He, J. Magn. Magn. Mater. **302**, 397 (2006). doi:10.1016/j.jmmm.2005.09.044

128. T.L.P. Dantas, V.P. Mendonca, H.J. Joséa, A.E. Rodriguesb, R.F.P.M. Moreira, Chem. Eng. J. **118**, 77 (2006)

129. S. Al-Sayari, A.F. Carley, S.H. Taylor, G.J. Hutchings, Top. Catal. **44**, 123 (2007). doi:10.1007/s11244-007-0285-9

130. G.J. Hutchings, M.S. Hall, A.F. Carley, P. Landon, B.E. Solsona, C.J. Kiely et al., J. Catal. **242**, 71 (2006). doi:10.1016/j.jcat.2006.06.001

131. J. Li, Y. Zhan, F. Zhang, X. Lin, Q. Zheng, Chinese J. Catal **29**, 346 (2008)

132. D. Andreeva, T. Tabakova, V. Idakiev, P. Christov, R. Giovanoli, Appl. Catal. A Gen. **169**, 9 (1998). doi:10.1016/S0926-860X(97)00302-5

133. Z. Wang, B. Shen, Z. Aihua, N. He, Chem. Eng. J. **113**, 27 (2005). doi:10.1016/j.cej.2005.08.003

134. K.M. Yao, S.I. Lee, Y.T. Lee, Y.K. Chung, I.S. Lee, Chem. Lett. **37**, 116 (2008). doi:10.1246/cl.2008.116

135. D.H. Zhang, G.D. Li, J.X. Li, J.S. Chen, Chem. Commun. (Camb) 3414 (2008). doi:10.1039/b805737k

136. A. Lu, E.L. Salabas, F. Schüth, Angew. Chem. Int. Ed. **46**, 1222 (2007). doi:10.1002/anie.200602866

137. M.D. Kaminski, L. Nuñez, J. Magn. Magn. Mater. **194**, 31 (1999). doi:10.1016/S0304-8853(98)00579-4

138. H.Y. Lin, Y.W. Chen, Ind. Eng. Chem. Res. **44**, 4569 (2005). doi:10.1021/ie0491488

139. G. Avgouropoulos, T. Ioannides, C. Papadopoulou, J. Batista, S. Hocevar, H.K. Matralis, Catal Today **75**, 157 (2002). doi:10.1016/S0920-5861(02)00058-5

140. Y.J. Jiang, J.H. Jiang, Q.M. Gao, M.L. Ruan, H.M. Yu, L.J. Qi, Nanotechnology **19**, 075714 (2008). doi:10.1088/0957-4484/19/7/075714

141. Z. Liu, D. Zhang, S. Han, C. Li, J. Am. Chem. Soc. **127**, 6 (2005). doi:10.1021/ja0445239

142. R.H.R. Castro, P. Hidalgo, J.A.H. Coaquira, J. Bettin, D. Zanchet, D. Gouvêa, Eur. J. Inorg. Chem. **11**, 2134 (2005). doi:10.1002/ejic.200400879

143. S. Decker, K.J. Klabunde, J. Am. Chem. Soc. **118**, 12465 (1996). doi:10.1021/ja962371e

144. C.L. Carnes, K.J. Klabunde, Chem. Mater. **14**, 1806 (2002). doi:10.1021/cm011588r

145. M.M. Natile, A. Glisenti, Chem. Mater. **15**, 2502 (2003). doi:10.1021/cm031019e

146. N.O. Nunez, P. Tartaj, M.P. Morales, P. Bonville, C.J. Serna, Chem. Mater. **16**, 3119 (2004). doi:10.1021/cm049860v

147. C.T. Chen, Y.C. Chen, Anal. Chem. **77**, 5912 (2008). doi:10.1021/ac050831t

148. C.T. Chen, Y.C. Chen, J. Biomed. Nanotechnol. **4**, 73 (2008). doi:10.1166/jbn.2008.008

149. Y. Li, Y. Liu, J. Tang, H. Lin, N. Yao, X. Shen et al., J. Chromatogr. A **1172**, 57 (2007). doi:10.1016/j.chroma.2007.09.062

150. R.Y. Hong, S.Z. Zhang, G.Q. Di, H.Z. Li, Y. Zheng, J. Ding et al., Mater. Res. Bull. **43**, 2457 (2008). doi:10.1016/j.materresbull.2007.07.035

151. J. Cheon, J. Park, J. Choi, Y. Jun, S. Kim, M.G. Kim et al., Proc. Natl. Acad. Sci. USA **103**, 3023 (2006). doi:10.1073/pnas.0508877103

152. D.S. Wang, J.B. He, N. Rosenzweig, Z. Rosenzweig, Nano. Lett. **4**, 409 (2004). doi:10.1021/nl035010n

153. Y. Li, J.S. Wu, D.W. Qi, X.Q. Xu, C.H. Deng, P.Y. Yang et al., Chem. Commun. (Camb) 564 (2008). doi:10.1039/b716055k

154. Y. Li, X.Q. Xu, D.W. Qi, C.H. Deng, P.Y. Yang, X.M. Zhang, J. Proteome. Res **7**, 2526 (2008). doi:10.1021/pr700582z

155. W.J. Chen, P.J. Tsai, Y.C. Chen, Small **4**, 485 (2008). doi:10.1002/smll.200701164

156. S. Laurent, D. Forge, M. Port, A. Roch, C. Robic, L.V. Elst et al., Chem. Rev. **108**, 2064 (2008). doi:10.1021/cr068445e